HUMAN ADENOVIRUS TYPE 37 AND THE BALB/C MOUSE: PROGRESS TOWARD A RESTRICTED ADENOVIRUS KERATITIS MODEL (AN AMERICAN OPHTHALMOLOGICAL SOCIETY THESIS)

BY James Chodosh MD

ABSTRACT

Purpose: To establish a mouse model of adenovirus keratitis in order to study innate immune mechanisms in the adenovirus-infected cornea.

Methods: Balb/c 3T3 fibroblasts were inoculated with human adenovirus (HAdV) serotypes 8, 19, or 37 and observed for cytopathic effect. Viral growth titers were performed, and apoptosis was measured by TUNEL assay. Viral and host cytokine gene expression was assessed by RT-PCR in cultured Balb/c 3T3 fibroblasts and in the corneas of virus-injected Balb/c mice. Western blot analysis was performed to detect cell signaling in the virus-infected cornea.

Results: Only HAdV37 induced cytopathic effect in mouse cells. Viral gene expression was limited, and viral replication was not detected. Apoptotic cell death in HAdV37-infected Balb/c cells was evident 48 and 72 hours postinfection ($P < .01$). MCP-1, IL-6, KC, and IP-10 mRNA levels were increased maximally by 8.4, 9.6, 10.5, and 20.0-fold, respectively, at 30 to 90 minutes after HAdV37 infection. Similar cytokine elevations were observed in the corneas of Balb/c mice 4 hours after stromal injection of HAdV37, when viral gene expression for the viral capsid protein IIIa was not detected. Western blot showed increased phosphorylation of ERK1/2 at 4 and 24 hours after corneal infection.

Conclusions: Despite limited viral gene expression, HAdV37 infection of Balb/c 3T3 fibroblasts results in increased proinflammatory gene expression. A similar pattern of cytokine expression in the corneas of HAdV37-infected Balb/c mice suggests the mouse adenoviral keratitis model may be useful for the study of early innate immune responses in the adenovirus-infected corneal stroma.

Trans Am Ophthalmol Soc 2006;104:346-365

INTRODUCTION

Ocular infection by subgroup D adenovirus (HAdV) serotypes 8, 19, or 37 causes epidemic keratoconjunctivitis (EKC), manifest by acute pseudomembranous conjunctivitis, punctate and macro-epithelial corneal erosions, and delayed-onset subepithelial corneal stromal infiltrates.[1] Subepithelial infiltrates, the hallmark of epidemic keratoconjunctivitis, cause photophobia, foreign body sensation, and reduced vision, and may persist and/or recur for months to years. It has been shown that HAdV19 infection of human corneal fibroblasts in vitro induces expression of the potent chemoattractants interleukin-8 (IL-8) and monocyte chemoattractant protein-1 (MCP-1), and that this expression appears to be transcriptionally regulated by an intracellular signaling cascade initiated by viral capsid binding to the cells.[2-5] These data suggest that adenoviral subepithelial corneal infiltrates result when infection of superficial keratocytes induces a specific intracellular signal transduction cascade leading to expression of proinflammatory mediators in the corneal stroma. However, a suitable animal model is lacking in which to confirm these observations. We hypothesize that the mouse cornea, while not intrinsically susceptible to infection with human adenoviruses, can serve as a suitable tissue site with which to study host-derived pathogenic mechanisms in adenovirus keratitis. Our long-term goal is to understand the interplay between adenoviruses and mechanisms of immunity in the human cornea. The specific purpose of this study was to determine whether mouse cells and/or the mouse cornea can be induced to express proinflammatory mediators upon infection with an ocular subgroup D adenovirus.

BACKGROUND AND SIGNIFICANCE

Ocular Adenovirus Infection

Originally isolated in 1953 from human adenoids,[6] the adenovirus is nonenveloped with a linear double-stranded DNA genome. The virus protein capsid forms a regular icosahedron with 20 triangular surfaces composed of 240 hexons, and 12 vertices each composed of a single penton. Each penton contains a penton base and a projecting fiber. DNA restriction enzyme analysis and genome typing has resulted in the classification of six adenovirus species or subgroups (A through F) containing a total of 51 distinct serotypes.

Most adenoviral eye disease presents clinically as one of three classic syndromes: simple follicular conjunctivitis, pharyngoconjunctival fever, or EKC. Serotypes 8, 19, and 37 (subgroup D) are the major etiologic agents of EKC, the only adenoviral syndrome with significant corneal involvement. In EKC, severe pseudomembranous conjunctivitis and punctate epithelial keratitis develop 1 week to 10 days after exposure, followed by multifocal subepithelial (stromal) corneal infiltrates 7 to 10 days thereafter. Subepithelial infiltrates, the *sine qua non* of EKC, cause photophobia and reduced vision and may persist for months to years.[7] Available evidence suggests that adenovirus infection of corneal cells plays a central role in the corneal manifestations of EKC. Others

From the Molecular Pathogenesis of Eye Infection Research Center, Dean A. McGee Eye Institute, Departments of Ophthalmology, Cell Biology, Microbiology, and Immunology, University of Oklahoma Health Sciences Center, Oklahoma City, Oklahoma. Supported in part by an unrestricted grant to the Department of Ophthalmology and a Physician-Scientist Award from Research to Prevent Blindness, New York, New York; and grants P30 EY012190, RO3 EY015222, and R01 EY013124 from the US Public Health Service. The author discloses no financial, proprietary, or commercial conflict of interest.

have shown that adenoviruses infect corneal epithelium and keratocytes in vitro and in vivo,[2,8-15] suggesting that adenoviral epithelial keratitis represents the clinical manifestation of viral cytopathic effect in the corneal epithelium, and that corneal subepithelial infiltrates in EKC might represent the effects of infection of keratocytes within the stroma.

Neutrophils are the first inflammatory cells in the tears of patients with EKC and the first cells to infiltrate the corneas of experimental animals with adenovirus keratitis.[16,17] Rare histopathologic specimens removed at surgery from patients with long-lasting subepithelial infiltrates due to EKC showed mononuclear cell infiltrates in the superficial corneal stroma.[18-20] Adenoviral particles were not apparent by electron microscopy,[19] nor was adenoviral antigen evident by immunofluorescence.[20] These anecdotal data are most consistent with the presence of a persistent chemotactic signal in the superficial corneal stroma long after viral replication has ceased and viral antigen has been consumed. In addition, the stromal location of infiltrates in the EKC-affected cornea suggests the possible participation by infected keratocytes in the inflammatory cascade. We hypothesize that keratocyte-derived leukocyte chemoattractants play a role in the pathogenesis of the stromal keratitis in EKC.

Human Keratocytes: Biology and Function

As the primary resident cells of the corneal stroma, keratocytes maintain the cornea in a precisely organized and transparent state.[21,22] Within the cornea, keratocytes are distinguishable as three distinct populations; those just beneath Bowman's membrane (subepithelial keratocytes) form a particularly dense cellular network,[23] contain twice as many mitochondria and considerably more heterochromatin than keratocytes in the mid and posterior regions.[22] Keratocytes capably produce mediators of inflammation, [24,25] including IL-6,[26] G-CSF, MCAF, MDNCF,[27] RANTES,[28] MIG, I-TAC, IP-10,[29] MCP-1,[28,30] GRO-α,[31] ENA-78,[27] and IL-8,[2-4,32,33] and have been implicated in necrotizing stromal inflammation due to herpes simplex virus[33] and gram-negative bacteria,[34,35] consistent with a role in stromal keratitis associated with infection by distinctly different pathogens. Proinflammatory gene expression by keratocytes may greatly exceed that of corneal epithelial cells.[2,28,32] In this regard, keratocytes are not unlike fibroblasts elsewhere in the body, in that they capably contribute to innate immune responses in tissue substantia propria.[36-41]

When liberated from the cornea and grown in the absence of serum, keratocytes express keratan sulfate proteoglycan and replicate slowly. Exposure of keratocytes to serum in culture induces a change to a fibroblast phenotype,[42,43] with increased assembly of stress fibers and focal adhesion complexes, and greater expression of fibronectin, collagen, and heparan sulfate. Injury to overlying corneal epithelium,[44] treatment with TGF-β,[45] or wounding[46] induces a myofibroblast phenotype, associated with expression of alpha-smooth muscle actin, and enhances the capacity to contract extracellular matrix.[47,48] The serum-dependent transformation from keratocyte to myofibroblast involves a phosphotyrosine signal transduction pathway[49] and may be at least partially reversible.[50] Owing to the effect of serum on keratocytes, they are generally referred to as corneal fibroblasts when cultured in serum-containing media. Although the keratocyte-fibroblast-myofibroblast paradigm is instructive, the normally avascular human cornea does contain serum components, albeit less so than tissues with a direct blood supply.[51] In addition, during the acute conjunctivitis in EKC, the superficial corneal stroma is bathed in serum factors present in conjunctival exudates.[7]

It is important to note that two separate laboratories—those of Hendricks[52] and Dana[53]—recently identified at least one and possibly several nonkeratocyte cell populations in the corneal stroma, including CD45+ CD11b+ leukocytes thought to be of the monocyte lineage. These cells can be isolated in culture by capture of the nonadherent cells that are typically discarded from keratocyte cultures (Pedram Hamrah, personal communication). How these resident leukocytes might contribute to innate immune mechanisms of inflammation in EKC remains unknown.

Intracellular Signaling Determines Adenovirus Entry Into Host Cells

Adenovirus infection of a susceptible cell begins with attachment of the penton fiber knob, the most distal component of the adenovirus capsid, to a specific receptor on the cell surface (Figure 1).[56] Known cellular binding sites for adenovirus fiber knob include the coxsackie-adenovirus receptor (CAR),[57] the α2 domain of MHC class I,[58] sialic acid,[59,60] and CD46 (membrane cofactor protein).[61-63] Recent evidence suggests that ocular pathogenic subgroup D adenoviruses bind to sialic acid or CD46.[64,65] This primary interaction facilitates an essential secondary interaction between Arg-Gly-Asp (RGD) motifs within the viral penton base protein on the proximal surface of the viral capsid and the cellular integrins $\alpha_v\beta_3$, $\alpha_v\beta_5$,[66] and $\alpha_v\beta_1$.[67] This requirement for integrin binding appears to be absolute for all adenoviruses except subgroup F.[68]

Integrins are heterodimeric transmembrane glycoproteins that orchestrate interactions between individual cells and the extracellular matrix and nearest cell neighbors.[69,70] Formed by the noncovalent association of one of 16 α subunits with one of eight β subunits,[71] integrins rely on interactions with secondary cytoplasmic proteins for the generation of downstream intracellular signaling. Integrin receptor occupation and clustering by a multivalent ligand[72,73] lead to rapid formation of focal adhesions within cells (the linking of integrins to intracellular cytoskeletal complexes and associated signaling proteins) and phosphorylation of intracellular tyrosine and serine-threonine kinases.

Binding of integrins by five RGD motifs on the adenovirus penton base optimally promotes integrin clustering in a five-sided ring[74] and initiates a signaling cascade necessary and sufficient for efficient virus internalization (Figure 1). In immortalized epithelial colon carcinoma (SW480) cells infected with HAdV2 (subgroup C), adenovirus internalization required the activation of phosphoinositide 3-kinase (PI3K),[55] and Rho family GTPases.[54] PI3K is a lipid kinase that catalyzes phosphorylation of phospholipid second messengers, that in turn activate the small GTP-binding proteins Ras, Rho, Rac, and CDC42.[75] Activated Rac and CDC42 induce actin polymerization,[76] and the end result is dynamin-dependent [77] viral internalization into endocytic vesicles via clathrin-coated pits.[78] Viral internalization, transport, and uncoating into the nucleus may occur within 2 hours of attachment to the cell.[79] The adenovirus replicative cycle that follows is divided into early (E) and late (L) phases with the late phase commencing with onset of

viral DNA replication. The early phase of adenovirus gene transcription has been further subdivided into "immediate early" (E1A), "delayed early" (E1B, E2A, E2B, E3, and E4), and "intermediate" (IVa2, IX) transcripts. In summary, adenovirus infection of target cells is an active cell-mediated process that requires intracellular signaling.

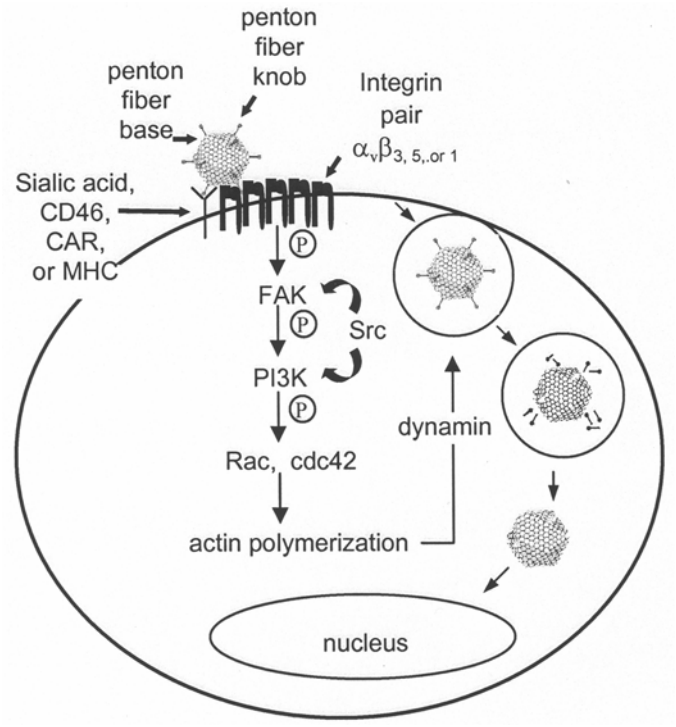

FIGURE 1

General schematic of adenovirus internalization cascade, based on studies performed with HAdV2 and SW480 cells.[54,55] After binding of the HAdV2 penton fiber knob to one of several possible primary receptors, a secondary interaction between the viral penton base and cellular integrins mediates activation of phosphoinositide 3-kinase (PI3K) and Rho GTPases. Subsequent dynamin-dependent actin polymerization induces clathrin-mediated endocytosis of viral particles.

Interleukin-8 and Monocyte Chemoattractant Protein-1: Paradigm Chemokines and Their Regulation

Chemokines are 8 to 10 kilodalton (k), basic, heparin-binding peptides with a four-cysteine motif that cause leukocyte chemotaxis with a high degree of specificity for leukocyte cell type.[80] Prior studies have suggested that the production of chemokines by adenovirus-infected tissues may be critical to the subsequent immunopathology associated with infection.[81] The α chemokines, known as CXC chemokines, contain one amino acid between the first and second cysteine, whereas the β or CC chemokines have adjacent cysteines. Interleukin-8 (IL-8, also known as CXCL8) is an α chemokine that strongly and selectively induces chemotaxis and degranulation of neutrophils with an exceptionally long duration of action, and to a lesser degree instigates chemotaxis of T lymphocytes.[82,83] Monocyte chemoattractant protein-1 (MCP-1, also known as CCL2), is a β chemokine that induces chemotaxis of monocytes, basophils, CD4+ and CD8+ lymphocytes, and T lymphocytes of the activated memory subset.[84]

Lipopolysaccharide treatment of keratocytes induces expression of both IL-8 and MCP-1.[85] Molecular regulation of IL-8 expression occurs largely at the transcriptional level via activation of latent transcription factors that bind to two distinct promoter regions in the 5′-flanking region of the IL-8 gene: a proximal region with adjacent binding sites for NF-κB and NF-IL6, and a distal binding site for AP-1.[86] The MCP-1 promoter contains two binding sites for NF-κB, and sites for AP-1 and Sp1 but not NF-IL6,[87,88] suggesting the potential for the differential regulation of these two chemokines. In viral infections, IL-8 expression may occur due to secondary oxidative stress,[86] early viral gene product activation of host gene transcription,[89,90] or protein kinase signaling cascades initiated by viral binding.[91,92] Early viral gene products can and do influence host gene expression during infection,[93,94] but once host cell machinery shuts down, viral gene products[95-97] cannot possibly influence transcription or translation of host genes.

Recent efforts toward understanding the pathogenesis of adenovirus keratitis have addressed the effects of cell signaling in HAdV19-infected human corneal fibroblasts and are summarized in Figure 2. Increased IL-8 expression upon HAdV19 infection of human corneal fibroblasts was shown to require host intracellular signaling but not viral gene or TNFα/IL-1β expression.[2-4] Increased MCP-1 mRNA and protein expression in HAdV19-infected human corneal fibroblasts, like IL-8, was shown to be dependent upon intracellular signaling.[4,5,98] These published findings using HAdV19 in human corneal fibroblasts were similar to those of Bruder and Kovesdi,[91] who showed that attachment of replication-defective HAdV5 (subgroup C) to HeLa cells led to phosphorylation of Raf-1 and ERK2 and downstream activation of IL-8 gene expression, suggesting a potential mechanism for the inflammation associated with adenoviral gene therapy.[100] Antiviral treatments targeted to viral replication and not viral binding to target cells, would not be expected to block chemokine expression due to viral attachment, suggesting that classic antiviral drugs would not prevent leukocyte infiltration into the cornea once epithelial infection is underway.

Chemokines can be extraordinarily resistant to degradation once bound by negatively charged proteins within extracellular matrix.[101] For example, IL-8 is extremely stable in tissues due to its propensity to bind to glycosaminoglycans.[102-105] When expressed into the cornea, IL-8 and MCP-1 likely bind to extracellular matrix components such as heparan sulfate at the corneal epithelial basement membrane to provide a degradation-resistant chemotactic signal that persists to some degree regardless of later events in infection.

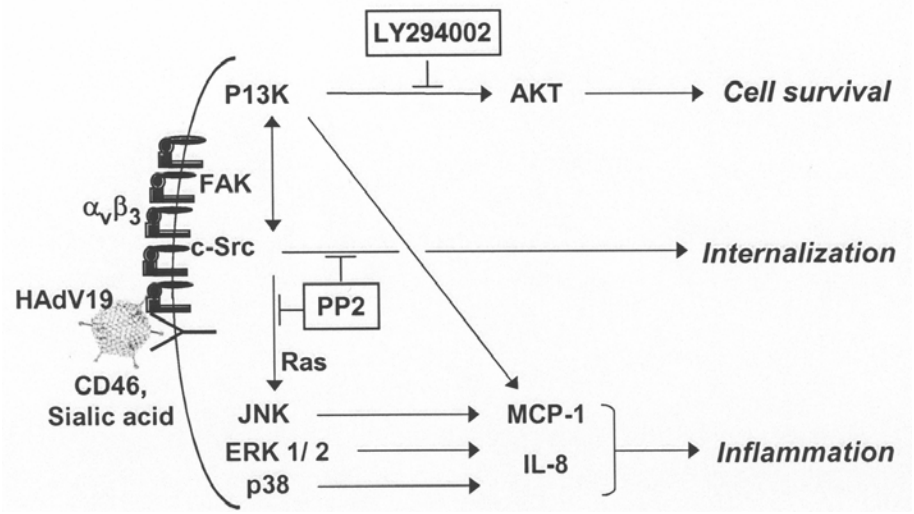

FIGURE 2

Model of cell signaling and downstream effects in HAdV19-infected human corneal fibroblasts.[2-5,98,99] Following primary and secondary binding to CD46 or sialic acid, and then $\alpha_v\beta_3$ integrin, respectively, the subgroup D adenovirus HAdV19 is internalized by the activity of Src kinase, leading to multiple downstream signaling events, and culminating in enhanced cell survival and proinflammatory gene expression.

Animal Models of Ocular Adenovirus Infection

Adenoviruses classically demonstrate a restricted host range; with few exceptions, human adenoviruses replicate poorly or not at all in nonhuman animals. Limited ocular infections with human isolates have been induced experimentally in the cotton rat[106] and the rabbit.[9,14,17,107-109] The cotton rat model was successfully utilized for the study of topical antivirals,[110] but was abandoned as a pathogenesis model for technical reasons. The rabbit model of ocular adenovirus infection has been used extensively for studies of antiviral therapy.[111-116] However, group D adenoviruses do not replicate in rabbits, and infection with group D adenoviruses does not induce keratitis.[108] Furthermore, the relative lack of species-specific reagents for immunologic studies in the cotton rat and rabbit models has made them impractical for study of immune responses to infection.

In contrast to other potential animals, the mouse has emerged as a favored model in which to study host-pathogen interactions.[117] Mouse cells are not susceptible to productive infection by human adenoviruses, but early viral gene expression was shown in human adenovirus-infected mouse 3T3 fibroblasts.[118] In these studies, the E1B 21k gene product, necessary for efficient viral DNA synthesis and protection of newly synthesized viral DNA against cell nucleases,[119-121] was not expressed, nor did viral replication occur. Despite such limitations, mouse models of several human adenovirus infections have been developed to study innate immune responses to the virus.[122-128] For example, infection of the mouse respiratory tract with human adenoviruses results in pneumonia,[129-132] despite limited viral gene expression.[133] In a fashion, the absence of adenoviral replication in the mouse has allowed investigators to analyze innate immune responses without the confounding influence of viral replication. Therefore, those wishing to study host-pathogen interactions in mice with human adenoviruses are either limited to or graced with (depending on one's perspective) experimental adenoviral pathogenesis models without the full repertoire of adenoviral gene and protein expression. This thesis will explore the consequences of infection of mouse cells by human adenoviruses and provide preliminary evidence for the feasibility of a mouse model for adenovirus keratitis.

METHODS

VIRUSES AND CELLS

Human adenovirus (HAdV) serotypes 8 and 37 were obtained from the American Type Culture Collection (ATCC, Manassas, Virginia) and grown in A549 cells (ATCC CCL 185, human lung carcinoma cells) in Minimum Essential Medium (MEM, Invitrogen, Carlsbad, California) with heat-inactivated 2% fetal bovine serum (FBS) and antibiotics. Four banked clinical EKC isolates of HAdV19 were used and cultured in similar fashion. After growth in A549 cells from the ATCC (American Type Culture Collection, Manassas, Virginia), viruses were cesium chloride gradient-purified and dialyzed against 10 mM Tris (pH 8.0) buffer with 80 mM NaCl, 2 mM $MgCl_2$, and 10% glycerol, titered in triplicate by the Tissue Culture Infectious Dose (TCID) assay, and stored at –80˚C. Balb/c 3T3 cells (clone A31- mouse embryo) were obtained from ATCC and cultured and maintained in Dulbeco's Modified Eagle's Minimum Essential Medium (DMEM) supplemented with heat-inactivated 10% FBS and antibiotics.

REAGENTS

SYBR green master mix for real-time PCR was purchased from Applied Biosystems, (Foster City, California). Other PCR reagents, including Taq polymerase, oligo dT (15mer) primers, and recombinant RNasin inhibitor, were obtained from Promega (Madison, Wisconsin). The Apotage peroxidase in situ apoptosis detection kit was obtained from Serological (Norcross, Georgia). Horseradish peroxidase-conjugated donkey anti-rabbit IgG and chemiluminescent reagents were obtained from Amersham (Piscataway, New Jersey). The polyclonal anti-phospho-ERK 1/2 antibody was obtained from Cell Signaling (Beverly, Massachusetts) and the polyclonal anti-total ERK 1/2 antibody was obtained from Promega.

IN VITRO VIRAL INFECTION

Balb/c 3T3 monolayer cultures were grown to ~ 95% confluence in six well culture plates, washed thrice with MEM 2% FBS, and infected with adenoviruses at multiplicities of infection (MOI) of 10 and 50 TCID/cell or mock infected with virus-free dialysis buffer. After 1 hour incubation at 37oC, the cells were washed gently, fed with MEM 2% FBS, and reincubated. Cell cultures were then observed for up to 28 days for the development of adenoviral cytopathic effect.

For growth titer experiments, 3T3 cells were grown in 48 well plates and infected or mock infected in triplicate for each time point. The cells and supernatants were harvested each day for 6 subsequent days postinfection, and titered. For viral and host gene expression experiments, RNA was harvested from mock and virus-infected cells as described below, at the indicated time points.

CORNEAL INJECTIONS

Balb/cJ mice aged 6 to 8 weeks were purchased from Jackson Labs (Bar Harbor, Maine) and maintained in strict accordance with institutional animal care facility guidelines and the ARVO Statement on the Use of Laboratory Animals in Ophthalmic Research. The animal protocol was approved by the University of Oklahoma Health Sciences Center Institutional Animal Care and Use Committee. Anesthesia was provided by intraperitoneal ketamine (80 mg/kg, Phoenix Scientific, St Joseph, Missouri) and xylazine (5 mg/kg, Bayer, Shawnee Mission, Kansas), followed by ocular topical application of proparacaine (0.5%, Allergan, Hormigueros, Puerto Rico). The right eye was gently prolapsed with curved forceps, and corneal injections were administered under a Zeiss OPMI VISU 140 Surgical Microscope (Thornwood, New York) with digital imaging system, using sterile glass needles heat-pulled from micropipettes, (Needle/Pipette Puller, Model 730, David Kopf Instruments, Tujunga, California, and KT Brown Type Micro-Pipette Beveler, Model BV-10, Sutter Instrument, Novato, California), and a CO_2-powered microinjection system (PM2000 Cell Microinjector, MicroData Instruments, Plainfield, New Jersey). Either 1 μL of the dialysis buffer used to dialyze the purified virus (mock-infected control) or an equal volume of cesium chloride gradient-purified HAdV37 was injected into the right cornea, with the left eye left untouched in all mice. The injection needle was placed in the paracentral stroma of each cornea, and transient whitening of the corneal stroma was used to indicate a successful injection. Confirmation of the injection site was obtained by analysis of injected corneas with light and confocal microscopy (data not shown). After euthanasia of mice at selected time points post-infection, corneas were removed using Vannas scissors (Katena, Denville, New Jersey), and placed into RNAlater (Ambion, Austin, Texas) for PCR analysis, or chilled PBS (pH 7.4) for protein studies.

RNA ISOLATION

For RNA isolation, the corneas were lysed in 1 mL of TRIzol reagent (Invitrogen, Carlsbad, California) using RNase free, disposable, Pellet Pestle (Kimble/Kontes, Vineland, New Jersey), and RNA was isolated as per the manufacturer's protocol. Proteins were removed by a chloroform extraction of the lysate. RNA was precipitated from the supernatant with ethanol, and the pellet was resuspended in Tris-EDTA (pH 8.0). RNasin (Promega) was added to the RNA solution to prevent RNase action. Contaminating DNA was removed by DNase I (Promega) treatment followed by a phenol/chloroform extraction and subsequent ethanol precipitation of the RNA. The RNA was resuspended at a concentration of 1 mg/mL in DEPC-treated water. A spectrophotometric reading at a wavelength of 260 nm was used to determine the concentration of RNA. The quality of each RNA sample was determined by calculating the ratio of optical density of each RNA sample at 260:280 nm; a ratio of approximately 1.8 indicated that samples contained only nondegraded RNA.

REVERSE TRANSCRIPTASE POLYMERASE CHAIN REACTION

For synthesis of cDNAs, 5 μg of total RNA was reverse transcribed with Moloney murine leukemia virus reverse transcriptase (Promega) using an oligo-dT 15mer (Promega) as the primer. The reaction mixture for the reverse transcription reaction was composed of 1.5 U/μL of RNaseIn, 50 mM Tris-HCl (pH 8.3), 75 mM KCl, 3 mM $MgCl_2$, 10 mM DTT, 500 μM dNTPs and 10 U/μL of reverse transcriptase. A reaction without reverse transcription, which was composed of all of the above reactants except for the reverse transcriptase, was run with each experiment to rule out the possibility of amplification of contaminating genomic DNA in the PCR reaction step.

For reverse transcriptase PCR (RT-PCR) amplification of adenoviral mRNAs, optimal primers (T_m about 45°C to 55°C; GC content range 55% to 60%; primer length 14 to 24mer) were designed using the Primer Macintosh software and verified for interprimer and intraprimer interactions and self-dimerization using the Primer3 and Integrated DNA Technology (Coralville, Iowa) calculator software. Primers for amplification of viral genes were designed using known sequences of human adenoviruses, as shown in Table 1. Two μL of the cDNA obtained by reverse transcription were used with the PCR reaction mixture composed of 50 mM Tris-HCl (pH 9.0), 50 mM NaCl, 10 mM $MgCl_2$, 200 μM dNTPs, 20 μg/μL primers and 1 U of Taq polymerase (Promega). Thin-

walled PCR reaction tubes were used for the reactions, and the assay was performed on a programmable thermo-minicycler (MJ Research, Waltham, Massachusetts) using one cycle that comprised a denaturation step at 96°C for 2 minutes followed by 30 cycles of 96°C for 1 minute and 68°C for 2 minutes. The final extension step was carried out at 72° C for 5 minutes. The amplification products were analyzed by gel electrophoresis in 1% agarose gels, and the sizes of the amplicons were verified by comparing them to the 100 bp DNA marker (GIBCO, Carlsbad, California).

TABLE 1. PRIMER PAIRS FOR RT-PCR DETECTION OF HADV37 MRNAS

VIRAL GENE*	SOURCE (HADV)	NUCLEOTIDES	PRODUCT (BASES)	SEQUENCES
E1A 10s	9[a]	18-35 331-310	314	5′CCT GCC TTC AAC TGT GCC3′ 5′GAA AAC CTT CCT CAT AAC ACCG3′
E1A 12s	9	18-35 551-532	534	5′CCT GCC TTC AAC TGT GCC3′ 5′CAG GTC CAA AGG TTC ATC CC3′
E1A 13s	9	78-99 373-354	296	5′CCA CTT CAT ACA CCG ACT CTG3′ 5′CAG GTC CAA AGG TTC ATC C3′
E1B 19k	9	79-98 491-474	413	5′TTC TGG AGA CAC TGG TTT GG 5′CTG CCT CAT TTC TTC CTC C
E1B 55k	9	309-325 513-495	205	5′GAG GGA GAG GAG CGA TG3′ 5′AAT AGC CTC CTC CCA ATC C3′
E3B 10.4k	37[b]	106-121 233-219	126	5′CCA ACC TAC CTC CTC T3′ 5′TCG GGA CTG TGA TGG 3′
E3B 14.5k	37	19-34 214-200	196	5′CTG CTA TCC CTC CTA T3′ 5′CGA GAT CAA AAC AGG3′
E3B 14.7k	37	116-130 282-268	167	5′TCA ACA TCC ACC AGT3′ 5′CTG GGT GAT GAC TAT G3′
E4	9[c]	139-155 362-346	224	5′AAA GTG AGT GTG CTG GT3′ 5′TCA CTC TCT CCA GCA AC3′
pIX	9[d]	78-98 233-216	156	5′AGT TCG TCA GAA TGT GAT GGG3′ 5′GCC AGT CTC GTC GCT GTC3′
IVa2	40[e]	398-417 499-480	102	5′ACC ACC AGC ACA GTG TAT CC3′ 5′AAA TCT CGG AGG CAA GG3′
L1 52, 55k	40	698-715 1126-1107	429	5′TCC TTC AGA GCA TTG TGG3′ 5′AGT CCT CCT CAT CTT CTT CC3′
L2 III	40	1034-1052 1417-1397	384	5′ACG GAG ATG CAG AGA AAG G3′ 5′GCT GAA CTC CAC TGA TAC TGC3′
L3 1	2[f]	1145-1164 1483-1464	339	5′TGA CAG AGG ACA GCA AGA AA3′ 5′CGT GGG TCA GAG AGG TAA AC3′
L5	2	1188-1207 1405-1386	218	5′TGA CAA ACT TAC CCT GTG GA3 5′CTC CAT TAG AAC ACC GTT TT3′

RT-PCR = reverse transcriptase polymerase chain reaction.
*Genbank accession numbers: a. AF099665; b. AF086569; c. SB2508; d. AF099665; e. NC_001454; f. NC_001405.

Quantitative real-time PCR analysis of viral and host gene expression in HAdV37 and buffer-injected corneas was performed using the RNA pooled from three corneas in each treatment group, using the ABI Prism 7700 Sequence detection System (PE Applied Biosystems, Foster City, California) according to the manufacturer's instructions. Primers for real-time PCR of viral and mouse mRNAs were designed using Primer Express Software (PE Applied Biosystems) and are shown in Tables 2 and 3, respectively. RNA concentrations of samples were normalized using quantification of GAPDH mRNA. Three μL of cDNA were subjected to real-time PCR amplification in a final volume of 50 μL containing 25 μL of 2X SYBR green master mix and 250 nM of specific forward and reverse primers. Amplification curves were generated by monitoring the fluorescence of SYBR Green I as a measure of incorporation into the amplified product. Samples were then analyzed by comparison of the number of PCR cycles required to reach the midpoint of

each amplification curve, or threshold cycle (C_T). Comparison of gene expression between two samples was performed after GAPDH normalization by calculating the *n*-fold difference in mRNA abundance using the formula $y = 2^{-x}$, where $x = (C_T$ of sample 1 – C_T of sample 2) and $y = (n$-fold difference in mRNA abundance). For each gene, a range of concentrations for both the forward and reverse primers allowed us to determine the combination with optimum amplification. Reactions lacking template were used to control for primer-dimer formation. To control for contamination by residual genomic DNA, reverse transcriptase-negative and nontemplate controls were run in parallel with each experiment.

TABLE 2. PRIMER PAIRS FOR REAL-TIME PCR DETECTION OF HADV37 MRNAS

VIRAL GENE*	SOURCE (HADV)	NUCLEOTIDES	PRODUCT (BASES)	SEQUENCES
E1A 10s	9	715- 735	91	5′GGA GGT AGA TGC CCA TGA TGA3′
		805- 784		5′GTT GGC TAT GTC AGC CTG AAG A3′
E1B 19k	9	17-41	92	5′GTG GAC TAT CCT TGC AGA CTT TAG C3′
		108-86		5′TTC CAA ACC AGT GTC TCC AGA AC3′
IIIa	17	1322-1342	104	5′ CCTTTCCTAGCTTAGGGAGTT3′
		1425-1405		5′CGAGTCGTTCAGGTACTCGTC3′

PCR = polymerase chain reaction.

*Genbank accession numbers: E1A 10S and E1B 19K: AF099665; IIIa: AF108105.

CYTOKINE QUANTIFICATION

For the quantification of cytokine proteins, corneas harvested at the specified times postinfection were dissected into 150 μL of chilled 1% SDS lysis buffer with protease inhibitors (10 μg/mL leupeptin, 1 mM phenylmethylsulphonylfluoride, and 10 μg/mL aprotonin), lysed using pellet pestle, and further homogenized by cold sonification (Sonic Dismembrator, Fisher, Pittsburgh, Pennsylvania). Supernatants were collected after centrifugation and the pooled proteins from three corneas for each condition and time point were analyzed by the Bio-Plex cytokine assay system (BioRad, Hercules, California) per the manufacturer's instructions.

DETECTION OF APOPTOSIS

Balb/c 3T3 cells were infected with purified HAdV37 or mock infected with virus free buffer, and then fixed at 12, 24, 48, or 72 hours postinfection with 1% paraformaldehyde. Terminal deoxynucleiotide transferase dUTP nick end labeling (TUNEL) analysis for DNA fragmentation was carried out using the TUNEL Apoptosis Detection Kit (Upstate Biotechnology, Lake Placid, New York), following the manufacturer's instructions. Each experimental condition was duplicated in three wells, and the number of apoptotic cells in 10 high-power fields in each well was counted in masked fashion and averaged. The means for each experimental condition were compared by ANOVA with Scheffe's multiple comparison test.

SDS-PAGE AND IMMUNOBLOT ANALYSIS

For preparation of protein lysates, untouched, buffer-, or HAdV37-injected corneas were homogenized in 250 μL of chilled lysis buffer consisting of phosphate buffered saline (PBS), 1% Triton X-100 and 2 mM EDTA, 0.2 mM sodium orthovanadate, along with protease inhibitors including phenylmethylsulfonyl fluoride (1 mM), leupeptin (1 μg/mL) and aprotonin (10 μg/mL), and freeze thawed once in liquid nitrogen. Samples were sonicated on ice for 5 to 10 seconds, followed by centrifugation at 13000 × *g* for 10 minutes at 4°C. Thirty micrograms of total protein from each supernatant was boiled in 2X sample buffer (BioRad 2X Laemmli buffer: 62.5 mM Tris HCl [pH 6.8], 2% SDS, 25% glycerol, 0.01% Bromophenol Blue, and 5% B-Mercaptoethanol) and immediately loaded on 10% SDS-PAGE. The resulting gels were transferred to nitrocellulose membranes using a BioRad Mini-Protean II transblot apparatus.

Nitrocellulose membranes were blocked overnight at 4°C in 4% bovine serum albumin. Incubation with primary antiserum was performed for 2 hours at room temperature. Immunoblots were washed thrice with Tris-buffered saline after both the primary and secondary incubations. Antibody reactivity was determined with enhanced chemiluminescent reagents (Amersham Biosciences, Piscataway, New Jersey), using the appropriate peroxidase conjugated secondary antibody.

REPETITION OF EXPERIMENTS AND STATISTICAL ANALYSIS

All experiments were performed at least three times. For statistical analysis when appropriate, the means from each experimental condition were compared by ANOVA with Scheffe's multiple comparison test, using SAS statistical software (Cary, North Carolina). $P < .01$ was considered significant.

RESULTS

HADV37 INDUCES CYTOPATHIC EFFECT IN MOUSE CELLS

At the onset of these studies, we sought to determine if a human adenovirus from subgroup D could be identified that would infect mouse cells in culture with the idea that such a virus would be the most likely to establish infection in the living mouse cornea. Cultured Balb/c 3T3 fibroblasts were seeded with HAdV8, 19 (four clinical isolates), or 37, at two different MOI (10 and 50 TCID/cell). Only HAdV37 infection at an MOI of 50 induced cytopathic effect, evident after 2 days and extensive at 3 days postinfection (Figure 3). Similar findings were seen in CRL cells, a Balb/c epithelioid cell line (ATCC) and Du17 cells, a C57BL/6J fibroblast cell line (provided courtesy of Dr Dusko Illic, data not shown). None of the other viruses tested induced cytopathic effect at these MOIs.

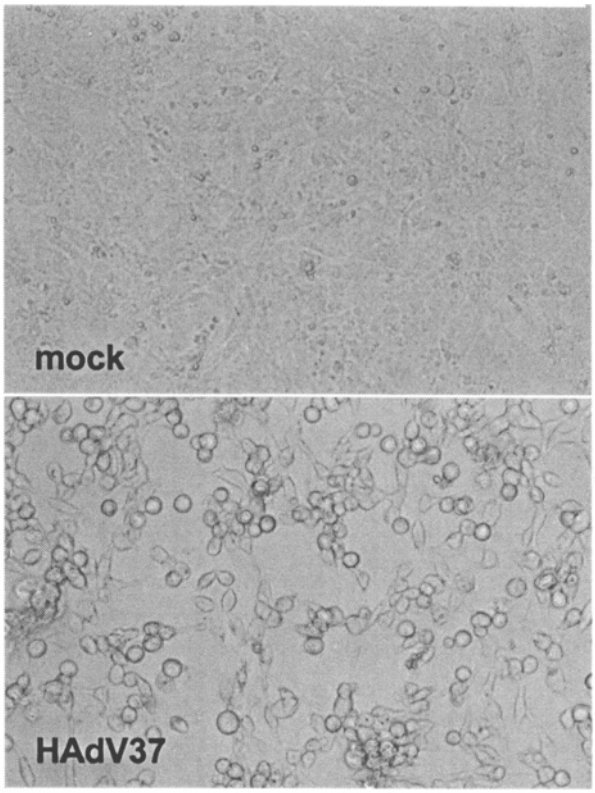

FIGURE 3

Cytopathic effect in Balb/c 3T3 fibroblasts observed at 72 hours after HAdV37 but not mock infection. Cells were infected at a multiplicity of infection of 50 TCID/cell and photographed with a Zeiss Axiovert inverted microscope (original magnification, ×200).

In light of the induction of apparent viral cytopathic effect in mouse cells upon infection with HAdV37, we then sought to determine whether the observed cell death was due to viral replication. Balb/c 3T3 cells were infected in triplicate with HAdV37 or buffer, and the cells and supernatants harvested each day for 6 subsequent days, and titered. The titer of HAdV37 fell steadily each day, from 57.0 TCID/cell immediately after infection to 1.5 TCID/cell on the sixth day postinfection (Figure 4), consistent with a lack of viral replication. Adenoviral capsids devoid of viral DNA can be produced in some adenovirus infections, and the empty capsids are toxic and induce cytopathic effect.[134] To test this alternate explanation for the viral cell death induced by HAdV37 in Balb/c 3T3 cells, we performed Western blot analysis comparing Balb/c 3T3 cultures after the development of cytopathic effect with those immediately after viral adsorption, but could not detect any increase in capsid protein (data not shown).

It has been suggested that the inability of human adenoviruses to replicate in mouse cells may be due to a failure to synthesize specific viral gene products.[118] We infected (human) A549 cells and Balb/c 3T3 fibroblasts in parallel, and performed RT-PCR at various times postinfection to detect expression of specific adenoviral genes. Although only a few regions of HAdV37 have been sequenced, we were able to use other published adenovirus sequences to develop primer pairs that would detect mRNA for HAdV37 genes in A549 cells (Table 1). Surprisingly, we found that HAdV37 gene expression did indeed take place in Balb/c 3T3 fibroblasts, although it typically occurred days rather than hours post-infection (Figure 5). For example, PCR products for the three E1A transcript sedimentation products examined (10s, 12s, and 13s) were evident at 2, 2, and 4 hours postinfection in A549 cells, but not until 48, 96, and 168 hours, respectively, in Balb/c cells. The same gene products are typically evident within 4 hours postinfection in human corneal fibroblasts (unpublished data). Furthermore, we could not detect some viral mRNAs at any time point in the mouse cells, including E3B 14.7k, E4, L1 52-55k, and L2 III. Interestingly, the 14.7k product of the E3B gene, with mRNA evident at 4 hours postinfection in A549 cells, protects adenovirus-infected cells against cytolysis by tumor necrosis factor (TNF).[135] Similarly, the failure of L1 52-55k gene to express in mouse cells—the transcript was noted in A549 cells at 6 hours postinfection—was also

noteworthy, because this gene product is essential to viral DNA encapsidation.[136] In contrast to our results with HAdV37, after infection with HAdV19 we could not detect any of the E1A sedimentation products in Balb/c 3T3 cells (data not shown), consistent with the observed failure to develop cytopathic effect after HAdV19 infection of mouse cells. Our data are consistent with internalization of HAdV37 into Balb/c 3T3 fibroblasts, and subsequent viral gene expression, albeit abortive. Whether HAdV19 or other noncytopathic HAdVs can be internalized in mouse cells but then fail to express early viral genes is not known.

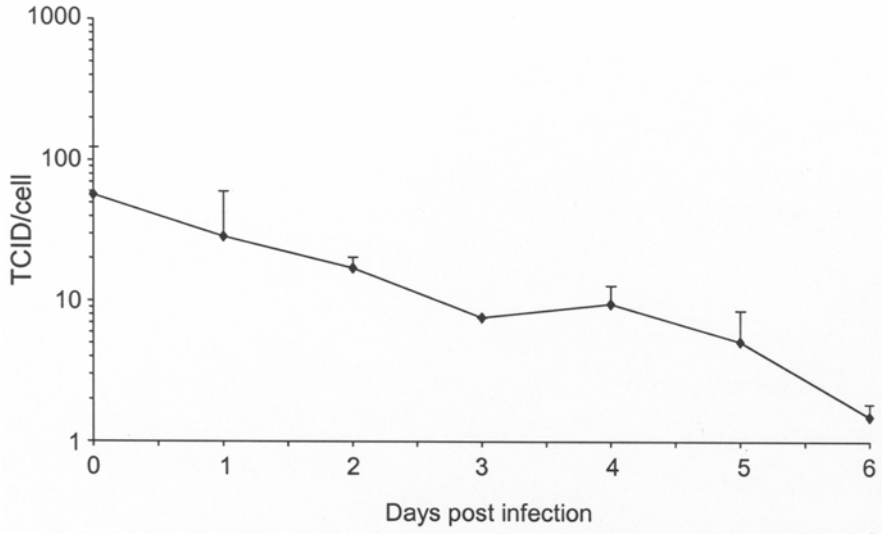

FIGURE 4

Growth curve for HAdV37 in Balb/c 3T3 fibroblasts. Cell monolayers at 95% confluence were infected in triplicate with HAdV37 at a multiplicity of infection of 50 TCID/cell, and cells and supernatants harvested daily for 6 days postinfection for titering. Error bars show the standard deviation of the mean titer at each time point.

FIGURE 5

Expression of specific HAdV37 mRNAs by reverse transcriptase polymerase chain reaction (RT-PCR) in Balb/c 3T3 cells (O) vs A549 cells (■). Cell monolayers at 95% confluence were infected in triplicate with HAdV37 at a multiplicity of infection (MOI) of 50 TCID/cell, and RNA harvested as described in the "Methods" section, and subjected to RT-PCR with primers listed in Table 1. The time of earliest detection of each adenoviral transcript in at least three independent experiments is shown for each cell type. Those genes with an asterisk (*) were found to be expressed only in the human A549 cells, not in the mouse cells.

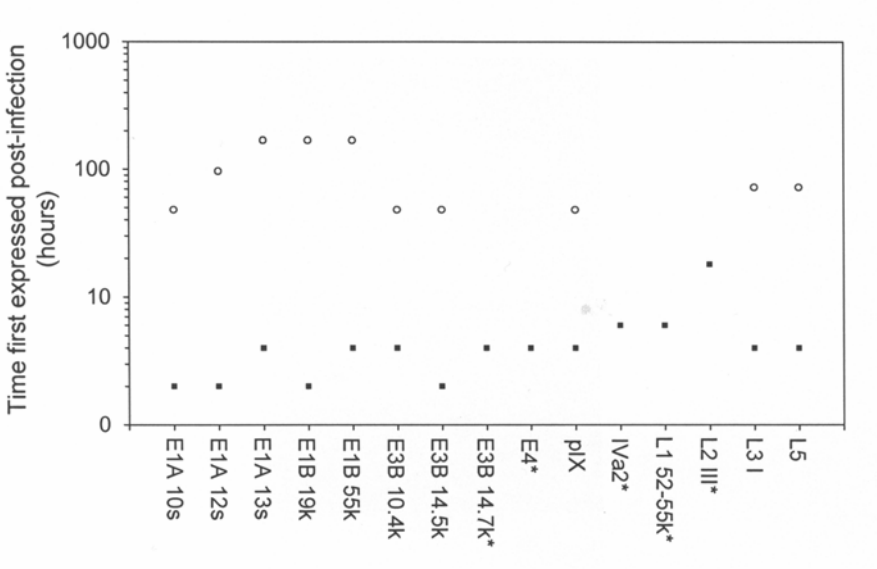

HADV37 INDUCES APOPTOTIC CELL DEATH IN MOUSE CELLS

To test the hypothesis that the cytopathic effect seen in mouse cells upon HAdV37 infection was due to apoptosis, Balb/c 3T3 fibroblasts were infected with HAdV37 or mock-infected with buffer in triplicate and fixed for TUNEL staining at 12 to 72 hours postinfection. As seen in Figure 6, at 48 and 72 hours postinfection, there was a significantly greater number of apoptotic cells in HAdV37-infected cell cultures than in mock-infected cultures (number of apoptotic cells/high-powered field for virus vs mock infection: 61.0 ± 7.3 vs 2.7 ± 0.9, and 44.7 ± 3.3 vs 8.7 ± 5.8, at 48 and 72 hours postinfection, respectively; $P < .01$ for 48- and 72-hour comparisons, ANOVA with Scheffe's multiple comparison test). We quantified the proportion of apoptotic cells per total cells, comparing mock- vs HAdV37-infected cells at these two time points. At 48 and 72 hours postinfection, the relative proportions were 1.3% vs 44.8%, and 11.8% vs 54.2%, respectively; similar findings were obtained in Du17 cells (data not shown).

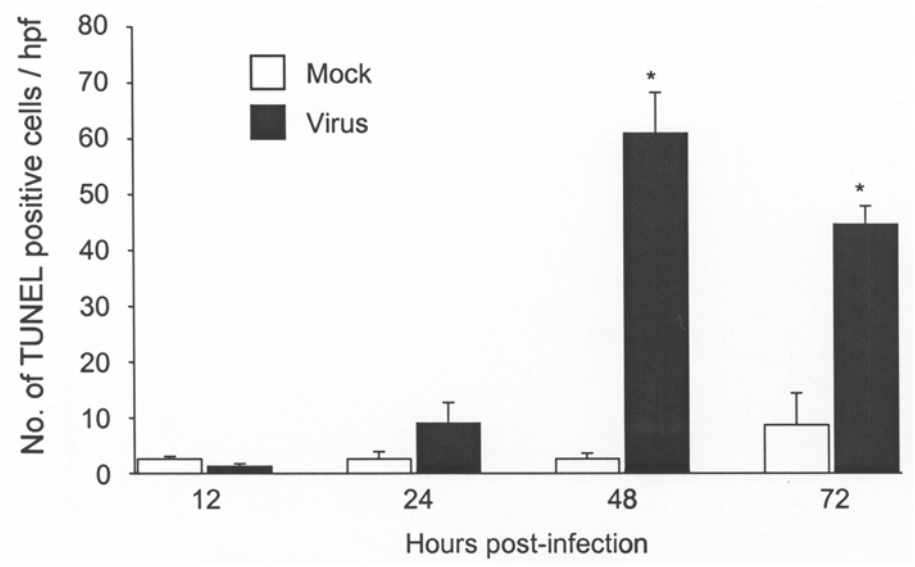

FIGURE 6

TUNEL-positive Balb/c 3T3 cells per high-powered field (hpf) at indicated times postinfection. Balb/c 3T3 fibroblasts were infected with buffer or HAdV37 at a multiplicity of infection of 50 TCID/cell. Significantly increased numbers of apoptotic cells were noted in HAdV37-infected cell cultures at 48 and 72 hours after infection, as compared to cells mock-infected with buffer (* $P < .01$). The experiment shown is representative of three independent experiments. Error bars show the standard deviation of the mean number of apoptotic cells at each time point.

HADV37 INDUCES PROINFLAMMATORY CYTOKINE EXPRESSION IN MOUSE CELLS

To determine whether HAdV37 infection of mouse cells was associated with induction of cytokine gene expression, real-time PCR was performed on HAdV37- and mock-infected Balb/c 3T3 cells. Cytokine mRNA levels were normalized by GAPDH, and the fold-difference between virus and mock-infected cells was determined as described in the "Methods" section, using the primers shown in Table 3. We chose four cytokines to examine, based on their possible importance in adenovirus keratitis. Interleukin-6 (IL-6) was studied because of its consistent induction in adenovirus infection in varied models.[130,137,138] The neutrophil chemokine and human IL-8 homolog, KC, was chosen because of evidence for IL-8 induction by adenovirus infection of human corneal cells,[2,4] and its similarity in function and regulation to human IL-8.[139-141] MCP-1 was selected because of studies that show it is upregulated in human corneal fibroblasts after HAdV19 infection.[4,5] IP-10, a CXC chemokine that attracts CD4+ T lymphocytes and has been shown to mediate a broad array of functions in viral infections,[142,143] was studied because of existing evidence for its role in inflammation associated with experimental adenovirus infections.[144-149] By real-time PCR, HAdV37 induced increased mRNA levels for all four cytokines at 30 minutes postinfection. Figure 7 shows one representative experiment of a total of three performed. While levels of KC and MCP-1 appear to have already peaked at or before 30 minutes postinfection with maximal fold-increases of mock-infected cells of 10.5 and 8.4, respectively, at 30 minutes, IL-6 and IP-10 mRNA levels appear to be increasing through the first 90 minutes, with fold-increases of 9.6 and 20.0, respectively, at 90 minutes postinfection.

TABLE 3. PRIMER PAIRS FOR REAL-TIME PCR DETECTION OF HOST MRNAS

MOUSE GENE*	NUCLEOTIDES	PRODUCT (BASES)	SEQUENCES
GAPDH	994-1020 1117-1093	124	5′GACAATGAATACGGCTACAGCAACAGG3′ 5′GTTGGGATAGGGCCTCTCTTGCTCA3′
KC	245-262 335-315	91	5′GCG CCT ATC GCC AAT GAG3′ 5′AGG GCA ACA CCT TCA AGC TCT3′
IL-6	136-158 226-208	91	5′CAC AGA GGA TAC CAC TCC CAA CA3′ 5′CAT TTC CAC GAT TTC CCA GAG A3′
MCP-1	345-366 435-416	91	5′GCC CTA AGG TCT TCA GCA CCT T3′ 5′TGC TTG AGG TGG TTG TGG AA3′
IP-10	146- 165 236- 216	91	5′GAT GAC GGG CCA GTG AGA AT3′ 5′TCG TGG CAA TGA TCT CAA CAC3′

PCR = polymerase chain reaction.

*Genbank accession numbers: GAPDH: BC083080; KC: U20527; IL-6: NM_031168; MCP-1: AF065931; IP-10: M33266.

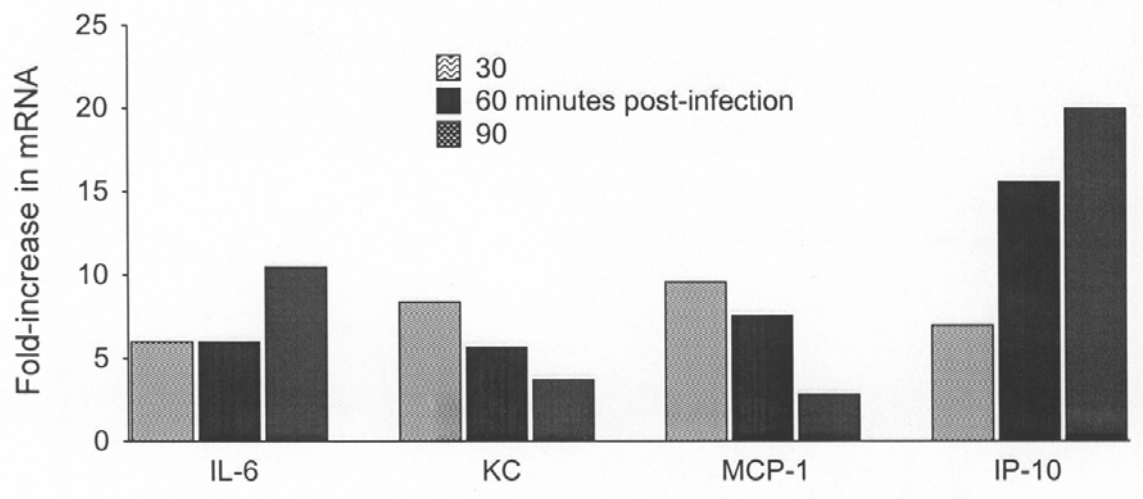

FIGURE 7

Real-time polymerase chain reaction (PCR) analysis of cytokine mRNA change induced in vitro by HAdV37 infection of Balb/c 3T3 fibroblasts. Cell monolayers were infected at a multiplicity of infection of 50 TCID/cell with HAdV37 or mock-infected with buffer and the RNA harvested at 30, 60, and 90 minutes postinfection. The height of each bar indicates the fold-increase in host cell cytokine gene expression induced at the indicated time after HAdV37 infection, as compared to mock-infected cells. Fold-increases in KC and MCP-1 mRNA expression appear maximal at 30 minutes postinfection, whereas fold-increases in IL-6 and IP-10 mRNA expression appear to be highest at 90 minutes postinfection. This experiment was repeated twice with similar results.

HADV37 INDUCES PROINFLAMMAMTORY CYTOKINE EXPRESSION IN THE BALB/C MOUSE CORNEA

Our in vitro data performed with cultured mouse cells strongly suggested the possibility that HAdV37, if properly applied to the mouse cornea, might induce inflammatory cytokines and thus allow the study of inflammatory gene expression in a mouse model of infection, even in the absence of viral replication. Our in vitro data was also consistent with other published studies showing that adenoviruses induce inflammation in living mice without viral replication.[126-133] We subsequently found that topical corneal application of HAdV37 to Balb/c mice without corneal scarification failed to induce changes in host gene expression, whereas infection with corneal scarification created too much of a local inflammatory response in controls to allow meaningful comparisons between groups at early time points (data not shown). When HAdV37 was injected into the cornea with a 33-gauge needle and Hamilton syringe, cytokine mRNA levels rose in both mock and HAdV37 injected mouse corneas in the first 4 to 8 hours, presumably due to the trauma of injection (data not shown). Finally, a less traumatic injection technique using sterile glass needles heat-pulled from micropipettes (see "Methods" section), and a CO_2-powered microinjection system was developed that induced only minimal alterations in cytokine gene expression in controls, thus allowing us to perform our analyses. The right corneas of anesthetized mice were injected in the midcorneal stroma with either 1 µL of the dialysis buffer used to dialyze the purified virus (mock-infected control) or with an equal volume of 10^8 TCID/mL, cesium chloride gradient-purified, HAdV37, and kept the left corneas as untouched controls. A successful corneal stomal injection was evident by transient whitening of the corneal stroma and confirmed by subsequent analysis of injected corneas with light and confocal microscopy (data not shown). Mice were euthanized at 4 hours postinjection, and three corneas in each treatment group were harvested and pooled for RNA extraction and subsequent real-time PCR for IL-6, KC, and IP-10. Fold-change in cytokine mRNA expression was determined in comparison to the quantity of mRNA for the same cytokine in untouched control corneas. At 4 hours postinfection, marked increases were noted in cytokine expression for all three cytokines (Figure 8), consistent with similar elevations at earlier time points in vitro for a panel of mediators similar to those elevated in HAdV37-infected mouse cells in vitro. Levels of fold-increase were 13.7, 25.6, and 12.9 for IL-6, KC, and IP-10, respectively, with a similar pattern of increase seen in two additional experiments. The small amount of RNA present in each mouse cornea allowed us to test only three cytokines at any one time, and MCP-1 was omitted from these analyses.

Because of the importance attributed to neutrophils in the acute inflammatory response to adenovirus infection,[2] we sought in particular to confirm the real-time PCR data for the neutrophil chemoattractant KC. For the quantification of KC protein, three corneas each were harvested at 0, 4, and 8 hours postinfection, and protein was extracted and pooled for analysis by the Bio-Plex cytokine assay (see "Methods" section). We found that changes in KC mRNA were mirrored by increases in KC protein expression (Figure 9) and that the level of KC in HAdV37-injected corneas appeared greatest at 8 hours postinjection. The amount of KC detected was 235.0 pg per virus-infected cornea vs 8.0 pg per mock-infected cornea at 8 hours postinfection, an approximately 30-fold increase. A smaller elevation of IL-6 (13-fold) protein was detected after 8 hours (data not shown); MCP-1 and IP-10 proteins were not evaluated. The KC experiment was performed three times with similar results.

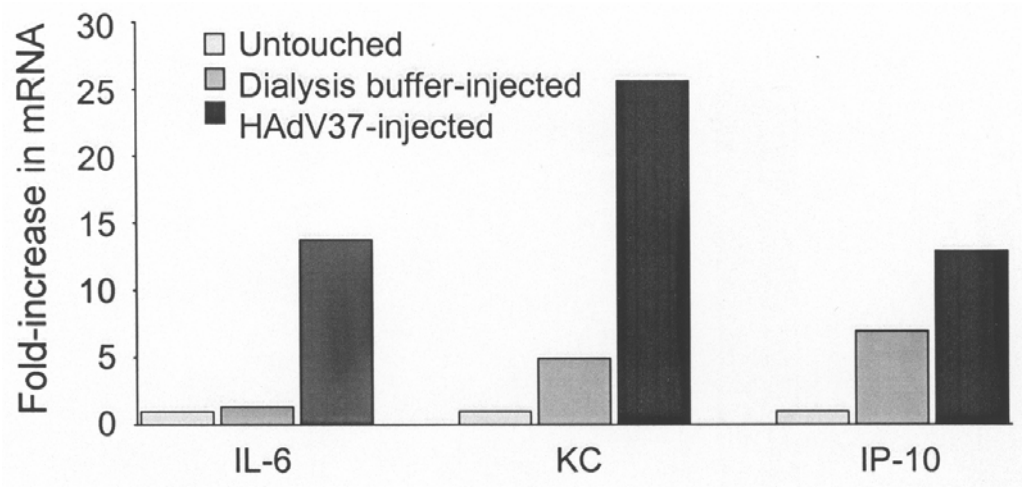

FIGURE 8

Real-time PCR analysis of change in host cytokine gene expression in Balb/c mice corneas at 4 hours after HAdV37 injection as compared to untouched and buffer-injected control corneas. The RNA from three corneas was pooled for analysis of each cytokine at each time point. The level of mRNA for each cytokine in buffer and HAdV37-injected corneas was expressed as the fold-increase over that of untouched corneas, set arbitrarily at a value of 1.0. mRNA levels for IL-6, KC, and IP-10 were all increased at 4 hours postinfection A similar pattern of increased expression for all three cytokines was seen in two replicates of this experiment.

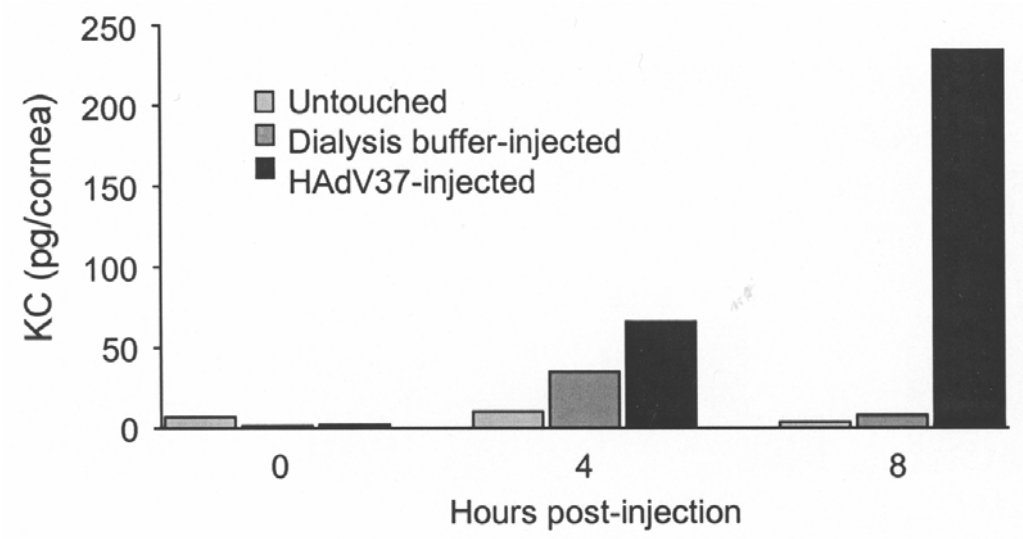

FIGURE 9

Analysis of KC protein expression in corneas of Balb/c mice at 0, 4, and 8 hours postinfection. Right corneas were injected with 10^8 TCID/ml of HAdV37 or buffer in 1 μL, and the left corneas used as untouched controls. Corneas were harvested at the specified times postinfection and dissected into chilled 1% SDS lysis buffer with protease inhibitors, lysed, and homogenized. Supernatants were collected after centrifugation, and KC protein quantity in each sample was analyzed by the Bio-Plex cytokine assay system and reported as the quantity of KC protein per cornea. KC levels were highest in HAdV37-injected corneas at 8 hours postinfection. This experiment was performed three times with equivalent results.

By real-time PCR performed on corneas at 4 hours postinjection, we also identified mRNA expression for E1A and E1B 19k HAdV37 genes but not IIIa (Figure 10), a late gene encoding a viral capsid protein, consistent with only early viral gene expression at a time when host proinflammatory gene expression is already upregulated. Because prior studies had demonstrated that host cytokine gene expression in HAdV19-infected human corneal fibroblasts was controlled by intracellular kinase activation events following viral binding to the cells,[3-5] we sought to determine whether cell signaling could be identified in the HAdV37-injected mouse cornea. Protein was harvested from corneas at 4 and 24 hours after injection of buffer or HAdV37 and subjected to Western blot for tyrosine phosphorylated and total ERK1/2, a tyrosine kinase shown previously to control induction of IL-8 gene expression in HAdV19-

infected corneal fibroblasts.[4] As shown in Figure 11, increased phosphorylation of ERK1/2 was seen at both time points in HAdV37-injected corneas as compared to buffer-injected corneas, consistent with enhanced tyrosine phosphorylation in virus-injected Balb/c corneas.

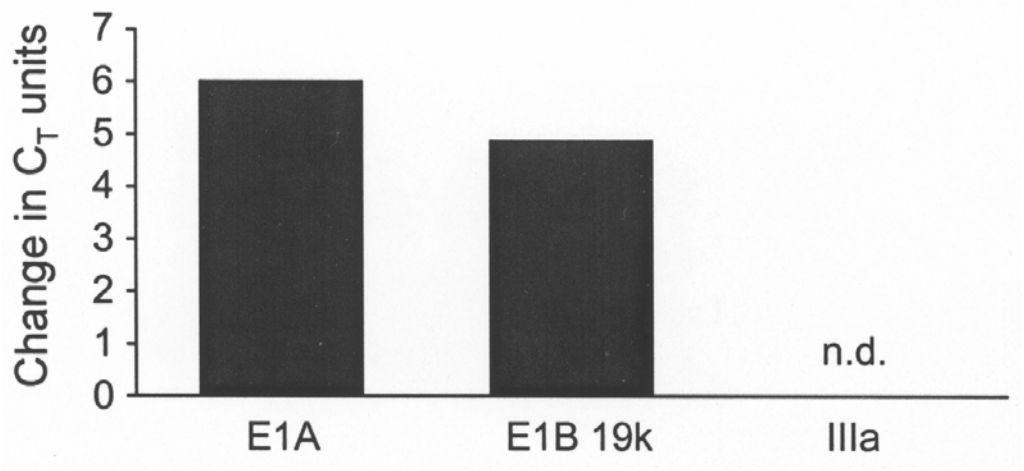

FIGURE 10

Real-time polymerase chain reaction (PCR) analysis for expression of adenoviral gene transcripts in corneas of Balb/c mice 4 hours after intrastromal injection with HAdV37. An increase in threshold cycle (C_T) units reflects an increase in the level of viral gene expression as compared to C_T levels obtained immediately after injection (before any viral gene expression has occurred). Viral mRNAs for E1A and E1B 19k transcripts were present in HAdV37-injected mouse corneas at 4 hours postinfection, but the IIIa viral capsid gene was not detected (n.d.) in the virus-infected cornea in any of three separate experiments at this time postinfection.

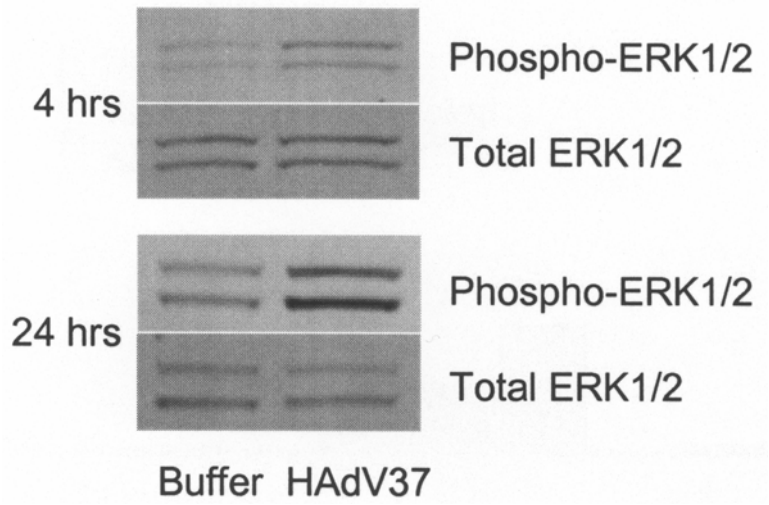

FIGURE 11

Immunoblot analysis for phosphorylation of ERK1/2 at 4 and 24 hours after HAdV37 injection into the corneas of Balb/c mice. HAdV37 or buffer was injected intrastromally at the indicated time points, and proteins from three corneas for each condition and time point were harvested and pooled for Western blot analysis. Each phospho-ERK blot (upper of each paired blot) was stripped and reprobed for total ERK (lower of each paired blot). Phosphorylation of ERK1/2 was increased at both 4 and 24 hours after infection with HAdV37 as compared to buffer-injected controls. No differences in total ERK1/2 levels were seen at either time point. This experiment was repeated twice with similar results.

DISCUSSION

Ocular infection by the subgroup D HAdV8, 19, or 37 has long been associated with EKC. Since Jones[150] first suggested almost 50 years ago that subepithelial stromal infiltrates in EKC might follow adenovirus infection of corneal epithelium, secondary viral antigen deposition in the superficial corneal stroma, and lymphocyte infiltration in a multifocal pattern at sites of antigen-antibody complexes, remarkably little progress has been made with regard to understanding the molecular pathogenesis of adenovirus keratitis. Experimental evidence for Jones' theory is still lacking, and we now know that antigen-antibody reactions in the cornea typically present as Wessely rings.[151]

Trousdale and coworkers' more recent finding that a nonreplicating adenovirus could induce subepithelial infiltrates when injected into the rabbit corneal stroma[17] showed that viral replication in the stroma was unnecessary for the development of stromal keratitis in EKC, but did not elucidate a specific molecular mechanism of inflammation. In an attempt to explain corneal stromal inflammation in

EKC as the outcome of the interaction between adenoviruses and resident cells of the corneal stroma, Chodosh and coworkers[2-5,99] demonstrated IL-8 and MCP-1 expression by HAdV19-infected keratocytes, and in a series of manuscripts showed that the production of these chemokines was induced by viral binding to the cells, followed by an intracellular signaling cascade leading ultimately to chemokine gene expression. In these studies, ultraviolet light inactivation of HAdV19 did not significantly reduce chemokine expression, whereas heat inactivation of the virus abrogated IL-8 expression, consistent with others' observations that binding of the virus to its target cell rather than viral replication might be the requisite step preceding corneal stromal inflammation in EKC. The observations of these latter two groups are consistent with one aspect of Jones' theory of subepithelial infiltrate formation: the presence of nonreplicating viral components in the corneal stroma may be sufficient to induce the necessary inflammatory signal. In this context, the obvious limitations of in vitro studies using human cells in monolayer culture and the limited availability of immunologic reagents for the rabbit model speak to the need for a mouse model of adenovirus keratitis with which to test such observations. The studies presented herein were designed to evaluate the possibility of development of just such a model.

In light of prior evidence that binding of adenoviruses to host cell target receptors was sufficient to initiate proinflammatory cytokine expression,[2,91] we set out to find a human adenovirus capable of binding and entering mouse cells. We chose to use BALB/c 3T3 fibroblasts, because of their availability and easy growth and maintenance, but confirmed our results in two other cell lines and a total of two mouse strains. Six different subgroup D adenoviruses were used, representing three different adenoviral serotypes, but only HAdV37 caused cytopathic effect in the mouse cells, evident as early as 3 days postinfection (Figure 3), but requiring a relatively high MOI. The infection of mouse cells by a human adenovirus is not completely without precedent. Eggerding and Pierce[118] demonstrated limited viral gene expression but not cytopathic effect after HAdV2 (subgroup C) infection of Balb/c 3T3 cells. Our growth curve (Figure 4) and viral gene expression studies (Figure 5) confirmed that HAdV37 entered the Balb/c cells and effected early viral gene expression, whereas the TUNEL assay (Figure 6) suggested that mouse cell death due to HAdV37 infection was secondary to apoptosis rather than productive infection and secondary cell lysis. Subsequent evaluation of proinflammatory gene expression in HAdV37-infected Balb/c 3T3 cells by real-time PCR showed that infection was associated with increased transcription of IL-6, KC, MCP-1, and IP-10 at 30 to 90 minutes postinfection (Figure 7), well before even early viral gene expression (Figure 5), suggesting that the transcription of cytokine genes in infected cells occurs despite delayed viral gene expression and in the absence of productive viral replication. These results are consistent with in vitro data in human corneal fibroblasts from Chodosh and coworkers, [2] in which host chemokine expression preceded HAdV19 gene expression. The apoptosis induced in three different mouse cell lines by HAdV37 was curious in light of the recent observation that HAdV19 infection of human corneal fibroblasts induces activation of the anti-apoptotic PI3K/Akt signaling pathway. Blockade of this pathway with genetic or chemical inhibitors results in increased apoptosis and reduced viral gene expression, perhaps owing to a lack of viable cells in which to replicate.[99] Why adenovirus infection of human cells results in prolongation of cell viability and enhancement of viral replication by the prevention of apoptosis, whereas infection of mouse cells leads to early apoptosis and a failure of viral replication, remains unknown, but may have to do with the receptors utilized for entry into the cell or with differences in cell signaling after entry. It is tempting to speculate that chemical or molecular inhibition of apoptosis in HAdV37-infected mouse cells might prolong cell viability and make them permissive for viral replication.

In light of the experimental evidence that viral binding rather than viral replication might be responsible for the stromal keratitis in EKC,[2] our principal goal was to develop a mouse model that would allow for the analysis of early molecular events in the cornea due to viral binding to resident stromal cells, without inducing secondary inflammation from the means of inoculation itself. When scarification and injection of virus-free buffer into the cornea with a metal needle each were shown to result in high background levels of proinflammatory gene expression, we turned to a novel injection method utilizing a fine glass micropipette needle and gas-powered microinjection system that allowed a relatively atraumatic injection of a small volume of virus or buffer directly into the mouse corneal stroma. The atraumatic nature of this system was confirmed by the relatively low level of cytokines expressed in buffer-injected corneas (Figures 8 and 9).

For these studies, we chose to evaluate a limited array of proinflammatory mediators in the HAdV37-injected Balb/c mouse cornea. Mice do not produce IL-8, but because of in vitro evidence that IL-8 might be important to the pathogenesis of EKC,[2] we focused on the neutrophil chemokine, KC, which is expressed by resident tissue fibroblasts after injury,[152] and is a close homolog for IL-8. Elevations of KC mRNA (Figure 8) and protein (Figure 9) were found at 4 to 8 hours after infection; these findings may allow the study of mechanisms for increased cytokine gene expression due to adenovirus infection. KC and other cytokines were upregulated despite the absence of viral capsid gene IIIa expression (Figure 10), consistent with a model of adenoviral inflammation in which viral replication is not an essential component.[100] At the same time, real-time PCR confirmation of early adenoviral gene expression in the living mouse cornea means that HAdV37 must have entered and infected resident cells in the cornea, albeit abortively. Our demonstration of ERK1/2 phosphorylation in virus- but not buffer-injected corneas (Figure 11) was consistent with the hypothesis previously put forth by Chodosh and associates in which inflammation in the corneal stroma after adenovirus infection occurs after activation of a keratocyte signal transduction cascade leading to host proinflammatory gene expression.[3-5,99] Our HAdV37 mouse model should allow testing of this hypothesis, assuming a way can be found to block specific signaling events in the mouse cornea. Systemic and local administration of protein kinase inhibitors has been shown to reduce neutrophil infiltration in other mouse models of acute inflammation,[153-157] suggesting that similar approaches might be successful in the cornea.

Our goal was to develop a model in which we could analyze early gene expression events resulting from the interactions between human adenoviruses and resident cells in the mouse cornea. The development of corneal infiltration by leukocytes after corneal infection would represent an unanticipated largesse, but at no time in the limited observation time (first 24 hours) did we recognize

corneal infiltrates or other clinical signs of inflammation in HAdV37-infected Balb/c corneas. Longer observation times after injection combined with immunohistochemical evaluation will be necessary to determine if increases in proinflammatory gene expression are accompanied by the eventual infiltration of leukocytes and the development of clinically recognizable keratitis. Possibly, as in other mouse infection models, strains of mice other than Balb/c might be more susceptible to infection,[158] and experiments are under way to determine if there is a better mouse strain in which to perform these experiments.

SUMMARY

This study focused on the development of a mouse model in which to study pathogenic mechanisms in adenovirus keratitis. Data was presented to show that HAdV37, an etiologic agent of EKC, infects mouse cells in vitro, where the virus undergoes limited viral gene expression, induces proinflammatory gene expression by host cells, and eventually kills the cells by apoptosis in the absence of viral replication. A novel means of mouse corneal infection was developed that allows for the atraumatic delivery of virus to the corneal stroma, where host proinflammatory gene and protein expression occurs along with tyrosine phosphorylation of a key protein kinase, despite delayed and ultimately incomplete viral gene expression.

ACKNOWLEDGMENTS

I wish to acknowledge the scientific contributions of Maitreyi S. Rajala PhD, Kanchana Natarajan PhD, Ashish V. Chintakuntlawar MBBS, Roger A. Astley, Tiaquanne Webb, and Jamie Meltzner.

REFERENCES

1. Gordon YJ, Aoki K, Kinchington PR. Adenovirus keratoconjunctivitis. In: Pepose JS, Holland GN, Wilhelmus KR, eds. *Ocular Infection & Immunity.* St Louis: Mosby; 1996; 877-894.
2. Chodosh J, Astley RA, Butler MG, Kennedy RC. Adenovirus keratitis: a role for interleukin-8. *Invest Ophthalmol Vis Sci* 2000;41:783-789.
3. Natarajan K, Ghalayini AJ, Sterling RS, Holbrook RM, et al. Activation of focal adhesion kinase in adenovirus-infected human corneal fibroblasts. *Invest Ophthalmol Vis Sci* 2002;43:2685-2690.
4. Natajaran K, Rajala M, Chodosh J. c-Src activation induces early IL-8 expression in adenovirus-infected human corneal fibroblasts. *J Immunol* 2003;170:6234-6243.
5. Xiao J, Chodosh J. JNK regulates MCP-1 expression by adenovirus type 19 infected human corneal fibroblasts. *Invest Ophthalmol Vis Sci* 2005;46:3777-3782.
6. Rowe WP, Heubner RJ, Gilmore LK, et al. Isolation of a cytopathogenic agent from human adenoids undergoing spontaneous degeneration in tissue culture. *Proc Soc Exp Biol Med* 1953;84:570-573.
7. Butt AL, Chodosh J. Adenoviral keratoconjunctivitis in a tertiary care eye clinic. *Cornea* 2006;25:199-202.
8. Boniuk M, Phillips CA, Friedman JB. Chronic adenovirus type 2 keratitis in man. *N Engl J Med* 1965;273:924-925.
9. Boniuk M, Phillips CA, Hines MJ, Friedman JB. Adenovirus infections of the conjunctiva and cornea. *Trans Am Acad Ophthalmol Otolaryngol* 1966;70:1016-1026.
10. Chodosh J, Miller D, Stroop WG, Pflugfelder SC. Adenovirus epithelial keratitis. *Cornea* 1995;14:167-174.
11. Dawson CR, Hanna L, Togni B. Adenovirus type 8 infection in the United States. IV. Observations on the pathogenesis of lesions in severe eye disease. *Arch Ophthalmol* 1972;87:258-268.
12. von Imre G, Korchmaros I, Opauszki A. Uber die keratoconjunctivitis epidemica. *Klin Monatsbl Augenheilkd* 1963;143:362-375.
13. Maugdal PC. Cytopathology of adenovirus keratitis by replica technique. *Br J Ophthalmol* 1990;74:670-675.
14. Schwartz HS, Yamashiroya HM. Adenovirus types 8 and 19 infection of rabbit corneal organ cultures. *Invest Ophthalmol Vis Sci* 1979;18:956-963.
15. Xiao J, Natarajan K, Rajala MS, et al. Vitronectin: a possible determinant of adenovirus type 19 tropism for human corneal epithelium. *Am J Ophthalmol* 2005;140:363-369.
16. Trousdale MD, Nobrega R, Stevenson D, et al. Role of adenovirus type 5 early region in the pathogenesis of ocular disease and cell culture infection. *Cornea* 1995;14:280-289.
17. Trousdale MD, Nobrega R, Wood RL, et al. Studies of adenovirus-induced eye disease in the rabbit model. *Invest Ophthalmol Vis Sci* 1995;36:2740-2748.
18. Gunther R. Pathologisch-anatomischer befund einer hornhaut bei keratitis epidemica. *Klin Monatsbl Augenheilkd* 1939;103:309-314.
19. Lund OE, Stefani FH. Corneal histology after epidemic keratoconjunctivitis. *Arch Ophthalmol* 1978;96:2085-2088.
20. Tullo AB, Ridgway AE, Lucas DR, Richmond S. Histopathology of adenovirus type 8 keratitis. *Cornea* 1987;6:234.
21. Maurice DM. The structure and transparency of the cornea. *J Physiol* 1957:136:263-286.
22. Muller LJ, Pels L, Vrensen GFJM. Novel aspects of the ultrastructural organization of human corneal keratocytes. *Invest Ophthalmol Vis Sci* 1995;36:2557-2567.
23. Poole CA, Brookes N, Clover GM. Keratocyte networks visualized in the living cornea using vital dyes. *J Cell Sci* 1993;106:685-692.

24. Elner VM, Strieter RM, Pavilack MA, et al. Human corneal interleukin-8. IL-1 and TNF-induced gene expression and secretion. *Am J Pathol* 1991;139:977-988.
25. Wilson SE, He YG, Lloyd SA. EGF, EGR receptor, basic FGF, TGF beta-1 and IL-1 alpha mRNA in human corneal epithelial cells and stromal fibroblasts. *Invest Ophthalmol Vis Sci* 1992;33:1756-1765.
26. Cubitt CL, Lausch RN, Oakes JE. Differences in interleukin-6 gene expression between cultured human corneal epithelial cells and keratocytes. *Invest Ophthalmol Vis Sci* 1995;36:330-336.
27. Hong JW, Liu JJ, Lee JS, et al. Proinflammatory chemokine induction in keratocytes and inflammatory cell infiltration into the cornea. *Invest Ophthalmol Vis Sci* 2001;42:2795-2803.
28. Tran MT, Tellaetxe-Isusi M, Elner V, et al. Proinflammatory cytokines induce RANTES and MCP-1 synthesis in human corneal keratocytes but not in corneal epithelial cells. *Invest Ophthalmol Vis Sci* 1996;37:987-996.
29. McInnis KA, Britain A, Lausch RN, Oakes JE. Synthesis of α-chemokines IP-10, I-TAC, and MIG are differentially regulated in human corneal keratocytes. *Invest Ophthalmol Vis Sci* 2005;46;1668-1674.
30. Bian ZM, Elner VM, Lukacs NW, et al. Glycated human serum albumin induces IL-8 and MCP-1 gene expression in human corneal keratocytes. *Curr Eye Res* 1998;17:65-72.
31. Cubitt CL, Lausch RN, Oakes JE. Differential induction of Gro-α gene expression in human corneal epithelial cells and keratocytes exposed to proinflammatory cytokines. *Invest Ophthalmol Vis Sci* 1997;38:1149-1158.
32. Cubitt CL, Tang Q, Monteiro CA, et al. IL-8 gene expression in cultures of human corneal epithelial cells and keratocytes. *Invest Ophthalmol Vis Sci* 1993;34:3199-3206.
33. Oakes JE, Monteiro CA, Cubitt CL, Lausch RN. Induction of interleukin-8 gene expression is associated with herpes simplex virus infection of human corneal keratocytes but not human corneal epithelial cells. *J Virol* 1993;67:4777-4784.
34. Dighiero P, Behar-Cohen F, Courtois Y, Goureau O. Expression of inducible nitric oxide synthase in bovine corneal endothelial cells and keratocytes in vitro after lipopolysaccharide and cytokines stimulation. *Invest Ophthalmol Vis Sci* 1997;38:2045-2052.
35. Matsumoto K, Shams NB, Hanninen LA, Kenyon KR. Cleavage and activation of corneal matrix metalloproteases by *Pseudomonas aeruginosa* proteases. *Invest Ophthalmol Vis Sci* 1993;34:1945-1953.
36. Alsalameh S, Firestein GS, Oez S, Kurrle R, et al. Regulation of granulocyte macrophage colony stimulating factor production by human articular chondrocytes. Induction by both tumor necrosis factor-alpha and interleukin 1, downregulation by transforming growth factor beta and upregulation by fibroblast growth factor. *J Rheumatol* 1994;21:993-1002.
37. Aupperle KR, Bennett BL, Boyle DL, et al. NF-κB regulation by IκB kinase in primary fibroblast-like synoviocytes. *J Immunol* 1999;163:427-433.
38. Burger JA, Zvaifler NJ, Tsukada N, Firestein GS, Kipps TJ. Fibroblast-like synoviocytes support B-cell pseudoemperipolesis via a stromal cell-derived factor-1- and CD106 (VCAM-1)-dependent mechanism. *J Clin Invest* 2001;107:305-315.
39. Garcia-Ramallo E, Marques T, Prats N, et al. Resident cell chemokine expression serves as the major mechanism for leukocyte recruitment during local inflammation. *J Immunol* 2002;169:6467-6473.
40. Inoue T, Hammaker D, Boyle DL, Firestein GS. Regulation of p38 MAPK by MAPK kinases 3 and 6 in fibroblast-like synoviocytes. *J Immunol* 2005;174:4301-4306.
41. Lusso P. Chemokines and viruses: the dearest enemies. *Virology* 2000;273:228-240.
42. Fini ME. Keratocyte and fibroblast phenotypes in the repairing cornea. *Prog Retin Eye Res* 1999;18:529-551.
43. Fini ME, Girard MT. The pattern of metalloproteinase expression by corneal fibroblasts is altered by passage in cell culture. *J Cell Sci* 1990;97:373-383.
44. Nakamura K, Kurosaka D, Yoshino M, et al. Injured corneal epithelial cells promote myodifferentiation of corneal fibroblasts. *Invest Ophthalmol Vis Sci* 2002;43:2603-2608.
45. Jester JV, Barry PA, Cavanagh HD, Petroll WM. Induction of α-smooth muscle actin (α-SM) expression and myofibroblast transformation in cultured keratocytes. *Cornea* 1996;15:505-516.
46. Jester JV, Petroll WM, Barry PA, Cavanagh HD. Expression of α-smooth muscle (α-SM) actin during corneal stromal wound healing. *Invest Ophthalmol Vis Sci* 1995;36:809-819.
47. Jester JV, Barry PA, Lind GJ, et al. Corneal keratocytes: in situ and in vitro organization of cytoskeletal contractile proteins. *Invest Ophthalmol Vis Sci* 1994;35:730-743.
48. Masur SK, Conors RJ, Cheung J K-H, Antobi S. Matrix adhesion characteristics of corneal myofibroblasts. *Invest Ophthalmol Vis Sci* 1999:40:904-910.
49. Jester JV, Huang J, Barry-Lane PA, et al. Transforming growth factor β-mediated corneal myofibroblast differentiation requires actin and fibronectin assembly. *Invest Ophthalmol Vis Sci* 1999;40:1959-1967.
50. Berryhill BL, Kader R, Kane B, et al. Partial restoration of the keratocyte phenotype to bovine keratocytes made fibroblastic by serum. *Invest Ophthalmol Vis Sci* 2002;43:3416-3421.
51. Nees DW, Fariss RN, Piatigorsky J. Serum albumin in mammalian cornea: implications for clinical application. *Invest Ophthalmol Vis Sci* 2003;44:3339-3345.
52. Birssette-Storkus CS, Reynolds SM, Lepisto AJ, Hendricks RL. Identification of a novel macrophage population in the normal mouse corneal stroma. *Invest Ophthalmol Vis Sci* 2002;43:2264-2271.
53. Hamrah P, Liu Y, Zhang Q, Dana MR. The corneal stroma is endowed with a significant number of resident dendritic cells. *Invest Ophthalmol Vis Sci* 2003;44:581-589.

54. Li E, Stupack D, Bokoch GM, Nemerow GR. Adenovirus endocytosis requires actin cytoskeleton reorganization mediated by Rho family GTPases. *J Virol* 1998;72:8806-8812.
55. Li E, Stupack D, Klemke R, et al. Adenovirus endocytosis via α_v integrins requires phosphoinositide-3-OH kinase. *J Virol* 1998;72:2055-2061.
56. Londberg-Holm K, Philipson L. Early events of virus-cell interactions in an adenovirus system. *J Virol* 1969;4:323-338.
57. Bergelson JM, Cunningham JA, Droguett G, et al. Isolation of a common receptor for coxsackie B viruses and adenoviruses 2 and 5. *Science* 1997;275:1320-1323.
58. Hong SS, Karayan L, Tournier J, et al. Adenovirus type 5 fiber knob binds to the MHC class I alpha-2 domain at the surface of human epithelial and B lymphoblastoid cells. *EMBO J* 1997;16:2294-2306.
59. Arnberg N, Edlund K, Kidd AH, Wadell G. Adenovirus type 37 uses sialic acid as a cellular receptor. *J Virol* 2000;74:42-48.
60. Arnberg N, Pring-Akerblom P, Wadell G. Adenovirus type 37 uses sialic acid as a cellular receptor on Chang C cells. *J Virol* 2002;76:8834-8841.
61. Gaggar A, Shayakhmetov DM, Lieber A. CD46 is a cellular receptor for group B adenoviruses. *Nat Med* 2003;9:1408-1412.
62. Segerman A, Atkinson JP, Marttila M, et al. Adenovirus type 11 uses CD46 as a cellular receptor. *J Virol* 2003;77:9183-9191.
63. Wu E, Trauger SA, Pache L, et al. Membrane cofactor protein is a receptor for adenoviruses associated with epidemic keratoconjunctivitis. *J Virol* 2004;78:3897-3905.
64. Wu E, Nemerow GR. Virus yoga: the role of flexibility in virus host cell recognition. *Trends Microbiol* 2004;12:162-169.
65. Zhang Y, Bergelson JM. Adenovirus receptors. *J Virol* 2005;79:12125-12131.
66. Nemerow GR, Stewart PL. Role of α_v integrins in adenovirus cell entry and gene delivery. *Microbiol Mol Biol Rev* 1999;63:725-734.
67. Li E, Brown SL, Stupack DG, et al. Integrin $\alpha_v\beta_1$ is an adenovirus coreceptor. *J Virol* 2001;75:5405-5409.
68. Mathias P, Galleno M, Nemerow GR. Interactions of soluble recombinant integrin $\alpha_v\beta_5$ with human adenoviruses. *J Virol* 1998;72:8669-8675.
69. Clark EA, Brugge JS. Integrins and signal transduction pathways: the road taken. *Science* 1995;268:233-239.
70. Kishimoto TK, Anderson DC. The role of integrins in inflammation. In: Gallin JI, Goldstein IM, Snyderman R, eds. *Inflammation: Basic Principles and Clinical Correlates.* 2nd ed. New York: Raven Press; 1992:353-406.
71. Hynes RO. Integrins: versatility, modulation, and signaling in cell adhesion. *Cell* 1992;69:11-25.
72. Miyamoto S, Akiyama SK, Yamada KM. Synergistic roles for receptor occupancy and aggregation in integrin transmembrane function. *Science* 1995;267:883-885.
73. Miyamoto S, Teramoto H, Coso OA, et al. Integrin function: molecular hierarchies of cytoskeletal and signaling molecules. *J Cell Biol* 1995;131:791-805.
74. Chiu CY, Mathias P, Nemerow GR, Stewart PL. Structure of adenovirus complexed with its internalization receptor, $\alpha_v\beta_5$. *J Virol* 1999;73:6759-6768.
75. Hall A. Rho GTPases and the actin cytoskeleton. *Science* 1998;279:509-514.
76. Nobes CD, Hall A. Rho, rac, and cdc42 GTPases regulate the assembly of multimolecular focal complexes associated with actin stress fibers, lamellipodia, and filopodia. *Cell* 1995;81:53-62.
77. Wang K, Huang S, Kapoor-Munshi A, Nemerow G. Adenovirus internalization and infection require dynamin. *J Virol* 1998;72:3455-3458.
78. Pastan I, Seth P, Fitzgerald D, Willingham M. Adenovirus entry into cells; some new observations on an old problem. In: Notkins A, Oldstone MBA, eds. *Concepts in Viral Pathogenesis*. New York: Springer-Verlag; 1987;141-146.
79. Horwitz MS. Adenoviridae and their replication. In: Fields BN, Knipe DM, eds. *Virology.* 2nd ed. New York: Raven Press; 1990:1679-1721.
80. Luster AD. Chemokines—chemotactic cytokines that mediate inflammation. *N Engl J Med* 1998;338:436-445.
81. Nazir SA, Metcalf JP. Innate immune response to adenovirus. *J Invest Med* 2005;53:292-304.
82. Baggiolini M, Dewald B, Walz A. Interleukin-8 and related chemotactic cytokines. In: Gallin JI, Goldstein IM, Snyderman R, eds. *Inflammation: Basic Principles and Clinical Correlates.* 2nd ed. New York: Raven Press; 1992:247-263.
83. Colditz IG, Zwahlen RD, Baggiolini M. Neutrophil accumulation and plasma leakage induced in vivo by neutrophil-activating peptide-I. *J Leukocyte Biol* 1990;48:129-137.
84. Carr MW, Roth SJ, Luther E, et al. Monocyte chemoattractant protein 1 acts as a T-lymphocyte chemoattractant. *Proc Natl Acad Sci U S A* 1994;91:3652-3656.
85. Kumagai N, Fukuda K, Fujitsu Y, et al. Lipopolysaccharide-induced expression of intercellular adhesion molecule-1 and chemokines in cultured human corneal fibroblasts. *Invest Ophthalmol Vis Sci* 2005;46:114-120.
86. Roebuck KA. Regulation of interleukin-8 gene expression. *J Interferon Cytokine Res* 1999;19:429-438.
87. Roebuck KA, Carpenter LR, Lakshminarayanan V, et al. Stimulus-specific regulation of chemokine expression involves differential activation of the redox-responsive transcription factors AP-1 and NF-κB. *J Leukoc Biol* 1999:65;291-298.
88. Ueda A, Okuda K, Ohno S, et al. NF-κB and SP1 regulate transcription of the human monocyte chemoattractant protein-1 gene. *J Immunol* 1994:153;2052-2063.
89. Fiedler MA, Wernke-Dollries K, Stark JM. Mechanism of RSV-induced IL-8 gene expression in A549 cells before viral replication. *Am J Physiol* 1996;271:L963-971.

90. Garofalo R, Sabry M, Jamaluddin M, et al. Transcriptional activation of the interleukin-8 gene by respiratory syncytial virus infection in alveolar epithelial cells: nuclear translocation of the RelA transcription factor as a mechanism producing airway mucosal inflammation. *J Virol* 1996;70:8773-8781.
91. Bruder JT, Kovesdi I. Adenovirus infection stimulates the Raf/MAPK signaling pathway and induces interleukin-8 expression. *J Virol* 1997;71:398-404.
92. Legastelois I, Levrey H, Greenland T, et al. Visna-maedi virus induces interleukin-8 in sheep alveolar macrophages through a tyrosine-kinase signaling pathway. *Am J Respir Cell Mol Biol* 1998;18:532-537.
93. Albrecht T, Boldagh I, Fons MP. Receptor-initiated activation of cells and their oncogenes by herpes-family viruses. *J Invest Dermatol* 1992;98:29S-35S.
94. Boldogh I, AbuBakar S, Albrecht T. Activation of proto-oncogenes: an immediate early event in human cytomegalovirus infection. *Science* 1990;24:561-564.
95. Hagmeyer BM, Angel P, van Dam H. Modulation of AP-1/ATF transcription factor activity by the adenovirus-E1A oncogene products. *Bioessays* 1995;17;621-629.
96. Keicho N, Elliott WM, Hogg JC, Hayashi S. Adenovirus E1A upregulates interleukin-8 expression induced by endotoxin in pulmonary epithelial cells. *Am J Physiol* 1997;272:L1046-1052.
97. Limbourg FP, Stadtler H, Chinnadurai G, et al. A hydrophobic region within the adenovirus E1B 19kDa protein is necessary for the transient inhibition of NF-κB activated by different stimuli. *J Biol Chem* 1996;271:20392-20398.
98. Natarajan K, Shepard LA, Chodosh J. The use of DNA array technology in studies of ocular viral pathogenesis. *DNA Cell Biol* 2002;21:483-490.
99. Rajala MS, Rajala RVS, Astley RA, et al. Corneal cell survival in adenovirus type 19 infection requires phosphoinositide 3-kinase/Akt activation. *J Virol* 2005;79:12322-12341.
100. Stephenson J. Studies illuminate cause of fatal reaction in gene-therapy trial. *JAMA* 2001;285:2570.
101. Witt DP, Lander AD. Differential binding of chemokines to glycosaminoglycan subpopulations. *Curr Biol* 1994;4:394-400.
102. Divietre JA, Smith MJ, Smith BRE, et al. Immobilized IL-8 triggers progressive activation of neutrophils rolling in vitro on P-selectin and intercellular adhesion molecule-1. *J Immunol* 2001;167:4017-4025.
103. Frevert CW, Kinsella MG, Vathanaprida C, et al. Binding of interleukin-8 to heparan sulfate and chondroitin sulfate in lung tissue. *Am J Respir Cell Mol Biol* 2003;28:464-472.
104. Middleton J, Neil S, Wintie J, et al. Transcytosis and surface presentation of IL-8 by venular endothelial cells. *Cell* 1997;91:385-395.
105. Webb LM, Ehrengruber MU, Clark-Lewis I, et al. Binding to heparan sulfate or heparin enhances neutrophil responses to interleukin-8. *Proc Natl Acad Sci U S A* 1993;90:7158-7162.
106. Tsai JC, Garlinghouse G, McDonnell PJ, Trousdale MD. An experimental model of adenovirus-induced ocular disease: the cotton rat. *Arch Ophthalmol* 1992;110:1167-1170.
107. De Hauwere B, Lutz A, Maudgal PC, et al. An ocular model of adenovirus type 5 infection in the rabbit. *Bull Soc Belge Ophthalmol* 1995;259:33-42.
108. Gordon YJ, Romanowski EG, Araullo-Cruz T. An ocular model of adenovirus type 5 infection in the NZ rabbit. *Invest Ophthalmol Vis Sci* 1992;33:574-580.
109. Romanowski EG, Araullo-Cruz T, Gordon YJ. Multiple adenoviral serotypes demonstrate host range extension in the New Zealand rabbit ocular model. *Invest Ophthalmol Vis Sci* 1998;39:532-536.
110. Kaneko H, Mori S, Suzuki O, et al. The cotton rat model for adenovirus ocular infection: antiviral activity of cidofovir. *Antiviral Res* 2004;61:63-66.
111. de Oliveira CB, Stevenson D, LaBree L, et al. Evaluation of Cidofovir (HPMPC, GS-504) against adenovirus type 5 infection in vitro and in a New Zealand rabbit ocular model. *Antiviral Res* 1996;31:165-172.
112. Gordon YJ, Romanowski EG, Araullo-Cruz T. Topical HPMPC inhibits adenovirus type 5 in the New Zealand rabbit ocular replication model. *Invest Ophthalmol Vis Sci* 1994;35:4135-4143.
113. Romanowski EG, Araullo-Cruz T, Gordon YJ. Topical corticosteroids reverse the antiviral effect of topical cidofovir in the Ad5-inoculated New Zealand rabbit ocular model. *Invest Ophthalmol Vis Sci* 1997;38:253-257.
114. Romanowski EG, Gordon YJ, Araullo-Cruz T, et al. The antiviral resistance and replication of cidofovir-resistant adenovirus variants in the New Zealand White rabbit ocular model. *Invest Ophthalmol Vis Sci* 2001;42:1812-1815.
115. Romanowski EG, Yates KA, Gordon YJ. Antiviral prophylaxis with twice daily topical cidofovir protects against challenge in the adenovirus type 5/New Zealand rabbit ocular model. *Antiviral Res* 2001;52:275-280.
116. Romanowski EG, Yates KA, Gordon YJ. Topical corticosteroids of limited potency promote adenovirus replication in the Ad5/NZW rabbit ocular model. *Cornea* 2002;21:289-291.
117. Buer J, Balling R. Mice, microbes and models of infection. *Nat Rev Genet* 2003;4:195-205.
118. Eggerding FA, Pierce WC. Molecular biology of adenovirus type 2 semipermissive infections. 1. Viral growth and expression of viral replicative functions during restricted adenovirus infection. *Virology* 1986;148:97-113.
119. Lai Fatt R, Mak S. Mapping of an adenovirus function in the inhibition of DNA degradation. *J Virol* 1982;42:969-977.
120. Pilder S, Logan J, Shenk T. Deletion of the gene encoding the adenovirus 5 early region 1B 21,000-molecular-weight polypeptide leads to degradation of viral and host cell DNA. *J Virol* 1984;52:664-671.

121. Subramanian T, Kuppuswamy M, Gysbers J, Mak S, Chinnadurai G. 19-kDa tumor antigen coded by early region E1b of adenovirus 2 is required for efficient synthesis and for protection of viral DNA. *J Biol Chem* 1984;259:11777-11783.
122. Day DB, Zachariades NA, Gooding LR. Cytolysis of adenovirus-infected murine fibroblasts by IFN-gamma-primed macrophages is TNF- and contact-dependent. *Cell Immunol* 1994;157:223-238.
123. Duerksen-Hughes PJ, Hermiston TW, Wold WS, Gooding LR. The amino-terminal portion of CD1 of the adenovirus E1A proteins is required to induce susceptibility to tumor necrosis factor cytolysis in adenovirus-infected mouse cells. *J Virol* 1991;65:1236-1244.
124. Gooding LR, Aquino L, Duerksen-Hughes PJ, et al. The E1B 19,000-molecular-weight protein of group C adenoviruses prevents tumor necrosis factor cytolysis of human cells but not of mouse cells. *J Virol* 1991;65:3083-3094.
125. Gooding LR, Ranheim TS, Tollefson AE, Aquino L, et al. The 10,400- and 14,500-dalton proteins encoded by region E3 of adenovirus function together to protect many but not all mouse cell lines against lysis by tumor necrosis factor. *J Virol* 1991;65:4114-4123.
126. Hayder H, Blanden RV, Korner H, et al. Adenovirus-induced liver pathology is mediated through TNF receptors I and II but is independent of TNF or lymphotoxin. *J Immunol* 1999;163:1516-1520.
127. Muruve DA. The innate immune response to adenovirus vectors. *Hum Gene Ther* 2004;15:1157-1166.
128. Rawle FC, Knowles BB, Ricciardi RP, et al. Specificity of the mouse cytotoxic T lymphocyte response to adenovirus 5. E1A is immunodominant in H-2b, but not in H-2d or H-2k mice. *J Immunol* 1991;146:3977-3984.
129. Ginsberg HS, Moldawer LL, Prince GA. Role of the type 5 adenovirus gene encoding the early region 1B 55-kDa protein in pulmonary pathogenesis. *Proc Natl Acad Sci U S A* 1999;96:10409-10411.
130. Ginsberg HS, Moldawer LL, Sehgal PB, et al. A mouse model for investigating the molecular pathogenesis of adenovirus pneumonia. *Proc Natl Acad Sci U S A* 1991;88:1651-1655.
131. Kajon AE, Gigliotti AP, Harrod KS. Acute inflammatory response and remodeling of airway epithelium after subspecies B1 human adenovirus infection of the mouse lower respiratory tract. *J Med Virol* 2003;71:233-244.
132. Sparer TE, Tripp RA, Dillehay DL, et al. The role of human adenovirus early region 3 proteins (gp19K, 10.4K, 14.5K, and 14.7K) in a murine pneumonia model. *J Virol* 1996;70:2431-2439.
133. Kafri T, Morgan D, Krahl T, et al. Cellular immune response to adenoviral vector infected cells does not require de novo viral gene expression: implications for gene therapy. *Proc Natl Acad Sci U S A* 1998;95:11377-11382.
134. Wigand R, Gelderblom H, Ozel M, et al. Characteristics of mastadenovirus h 8, the causative agent of epidemic keratoconjunctivitis. *Arch Virol* 1983;76:307-319.
135. Gooding LR, Elmore LW, Tollefson AE, et al. A 14,700 MW protein from the E3 region of adenovirus inhibits cytolysis by tumor necrosis factor. *Cell* 1988;53:341-346.
136. Gustin KE, Imperiale MJ. Encapsidation of viral DNA requires the adenovirus L1 52/55-kilodalton protein. *J Virol* 1998;72:7860-7870.
137. Benihoud K, Salone B, Esselin S, et al. The role of IL-6 in the inflammatory and humoral response to adenoviral vectors. *J Gene Med* 2000;2:194-203.
138. Kawasaki Y, Hosoya M, Katayose M, Suzuki H. Correlation between serum interleukin 6 and C-reactive protein concentrations in patients with adenoviral respiratory infection. *Pediatr Infect Dis* J 2002;21:370-374.
139. Ohmori Y, Fukumoto S, Hamilton TA. Two structurally distinct kappa B sequence motifs cooperatively control LPS-induced KC gene transcription in mouse macrophages. *J Immunol* 1995;155:3593-3600.
140. Ouaaz F, Li M, Beg AA. A critical role for the RelA subunit of nuclear factor kappaB in regulation of multiple immune-response genes and in Fas-induced cell death. *J Exp Med* 1999;189:999-1004.
141. Zhai Q, Luo Y, Zhang Y, et al. Low nuclear levels of nuclear factor-kappa B are essential for KC self-induction in astrocytes: requirements for shuttling and phosphorylation. *Glia* 2004;48:327-336.
142. Farber JM. Mig and IP-10: CXC chemokines that target lymphocytes. *J Leukoc Biol* 1997;61:246-257.
143. Neville LF, Mathiak G, Bagasra O. The immunobiology of interferon-gamma inducible protein 10 kD (IP-10): a novel, pleiotropic member of the C-X-C chemokine superfamily. *Cytokine Growth Factor Rev* 1997;8:207-219.
144. Borgland SL, Bowen GP, Wong NC, et al. Adenovirus vector-induced expression of the C-X-C chemokine IP-10 is mediated through capsid-dependent activation of NF-kappaB. *J Virol* 2000;74:3941-3947.
145. Charles PC, Chen X, Horwitz MS, Brosnan CF. Differential chemokine induction by the mouse adenovirus type-1 in the central nervous system of susceptible and resistant strains of mice. *J Neurovirol* 1999;5:55-64.
146. Liu Q, White LR, Clark SA, et al. Akt/protein kinase B activation by adenovirus vectors contributes to NFkappaB-dependent CXCL10 expression. *J Virol* 2005;79:14507-14515.
147. Muruve DA, Barnes MJ, Stillman IE, Libermann TA. Adenoviral gene therapy leads to rapid induction of multiple chemokines and acute neutrophil-dependent hepatic injury in vivo. *Hum Gene Ther* 1999;10:965-976.
148. Tibbles LA, Spurrell JC, Bowen GP, et al. Activation of p38 and ERK signaling during adenovirus vector cell entry lead to expression of the C-X-C chemokine IP-10. *J Virol* 2002;76:1559-1568.
149. Zeng X, Moore TA, Newstead MW, et al. IP-10 mediates selective mononuclear cell accumulation and activation in response to intrapulmonary transgenic expression and during adenovirus-induced pulmonary inflammation. *J Interferon Cytokine Res* 2005;25:103-112.

150. Jones BR. The clinical features of viral keratitis and a concept of their pathogenesis. *Proc Royal Soc Med* 1958;51:13-20.
151. Meyers-Elliott RH, Pettit TH, Maxwell WA. Viral antigens in the immune ring of herpes simplex stromal keratitis. *Arch Ophthalmol* 1980;98:897-904.
152. Armstrong DA, Major JA, Chudyk A, Hamilton TA. Neutrophil chemoattractant genes KC and MIP-2 are expressed in different cell populations at sites of surgical injury. *J Leukoc Biol* 2004;75:641-648.
153. Arndt PG, Young SK, Lieber JG, et al. Inhibition of c-Jun N-terminal kinase limits lipopolysaccharide-induced pulmonary neutrophil influx. *Am J Respir Crit Care Med* 2005;171:978-986.
154. Arndt PG, Young SK, Worthen GS. Regulation of lipopolysaccharide-induced lung inflammation by plasminogen activator inhibitor-1 through a JNK-mediated pathway. *J Immunol* 2005;175:4049-4059.
155. Ishii M, Suzuki Y, Takeshita K, et al. Inhibition of c-Jun NH2-terminal kinase activity improves ischemia/reperfusion injury in rat lungs. *J Immunol* 2004;172:2569-2577.
156. Kang JL, Lee HW, Lee HS, et al. Genistein prevents nuclear factor-kappa B activation and acute lung injury induced by lipopolysaccharide. *Am J Respir Crit Care Med* 2001;164:2206-2212.
157. Nick JA, Young SK, Arndt PG, et al. Selective suppression of neutrophil accumulation in ongoing pulmonary inflammation by systemic inhibition of p38 mitogen-activated protein kinase. *J Immunol* 2002;169:5260-5269.
158. Hazlett LD. Role of innate and adaptive immunity in the pathogenesis of keratitis. *Ocul Immunol Inflamm* 2005;13:133-138.